

1 **Inhalable textile microplastic fibers impair airway epithelial growth**

2
3 **Short title: Textile microplastic fibers impair organoid growth**

4
5
6 F. van Dijk^{1,2}, S. Song^{1,3}, G.W.A van Eck¹, X. Wu^{1,2}, I.S.T. Bos¹, D.H.A. Boom⁴, I.M.
7 Kooter⁴, D.C.J. Spierings⁵, R. Wardenaar⁵, M. Cole⁶, A. Salvati⁷, R. Gosens^{1,2}, B.N.
8 Melgert^{1,2,*}

9
10 ¹Groningen Research Institute for Pharmacy, Department of Molecular Pharmacology,
11 University of Groningen, Groningen, the Netherlands.

12 ²Groningen Research Institute for Asthma and COPD, University Medical Center Groningen,
13 University of Groningen, Groningen, the Netherlands.

14 ³Groningen Research Institute for Pharmacy, Department of Chemical and Pharmaceutical
15 Biology, University of Groningen, Groningen, the Netherlands.

16 ⁴The Netherlands Organization for Applied Scientific Research, TNO, Utrecht, the
17 Netherlands.

18 ⁵European Research Institute for the Biology of Ageing, University Medical Center
19 Groningen, University of Groningen, Groningen, the Netherlands.

20 ⁶Plymouth Marine Laboratory, Plymouth, United Kingdom.

21 ⁷Groningen Research Institute for Pharmacy, Department of Nanomedicine & Drug
22 Targeting, University of Groningen, Groningen, the Netherlands.

23
24 * Corresponding author:

25 Prof Dr Barbro N. Melgert

26 Groningen Research Institute of Pharmacy

27 Department of Molecular Pharmacology

28 University of Groningen

29 A. Deusinglaan 1

30 9713 AV Groningen

31 the Netherlands

32 b.n.melgert@rug.nl

33 **Abstract**

34 Synthetic textiles shed fibers that accumulate indoors and this results in continuous
35 exposure when indoors. High exposure to microplastic fibers in nylon flock workers has
36 been linked to the development of airway and interstitial lung disease, but the exact health
37 effects of microplastic fibers on the lungs are unknown. Here we determined effects of
38 polyester and nylon textile microplastic fibers on airway and alveolar epithelial cells using
39 human and murine lung organoids. We observed that particularly nylon microfibers had a
40 negative impact on the growth and development of airway organoids. We demonstrated that
41 this effect was mediated by components leaking from nylon. Moreover, our data suggested
42 that microplastic textile fibers may especially harm the developing airways or airways
43 undergoing repair. Our results call for a need to assess exposure and inhalation levels in
44 indoor environments to accurately determine the actual risk of these fibers to human health.

45
46
47 **Teaser**

48 Airborne fibers shed from synthetic textiles, in particular nylon, can inhibit repair of the cells
49 coating the airways

50

51 **Introduction**

52 Plastic pollution is a pressing global concern and microplastics are a significant part of this
53 problem (1). High amounts of microplastics have been found in marine environments, air,
54 soils, plants, and animals, which illustrates how omnipresent this relatively recent pollution
55 actually is (2). Microplastic pollution derives from personal care products, synthetic clothes,
56 and degradation of macroplastics (3, 4). Synthetic textile fibers are one of the most
57 prevalent types of microplastic waste observed, with an annual production of 60 million
58 metric tons, which equals 16% of the world's plastic pollution (1). These fibers are typically
59 composed of nylon or polyester and are released into the environment by wear and tear and
60 during washing and drying of garments (4-6).

61 The ubiquitous nature of microplastics in the environment inevitably leads to human
62 exposure, which can occur through two main routes (7, 8). Firstly, through ingestion of
63 contaminated food and water and secondly via inhalation. Microplastics have been reported
64 both in indoor and outdoor air, with levels indoors being 2-5 times higher as compared to
65 outdoors (9, 10). Whether or not microfibers can deposit in lung tissue largely depends on
66 the aerodynamic diameter of the fibers (7, 11). Lung deposition is most efficiently achieved
67 with aerodynamic diameters between 1-10 μm (12), however, these sizes are difficult to
68 quantify in environmental samples due to limitations of the analytical techniques (9, 13).
69 Yet, plastic microfibers have been found in human lung tissue, suggesting inhalation does
70 indeed take place (14). Furthermore, several studies from workers in synthetic textile, flock
71 and (poly)vinyl chloride industries suggest that inhalation of such microfibers is harmful, as
72 around 30% of factory workers developed work-related airway and interstitial lung disease
73 (15-23). Moreover, exposure to particulate matter in air pollution, also containing
74 microplastics (24-26), has been associated with higher risk of developing asthma and an
75 increase in asthma symptoms in areas with higher levels of particulate matter air pollution
76 (27-29).

77 Despite the potential capacity for microplastic fibers to contribute to respiratory diseases,
78 the health effects are greatly understudied and information providing evidence of potential
79 human health effects of inhaled microplastics is lacking (9, 30, 31). In the present study, we
80 therefore explored whether textile microplastic fibers can cause damage to lung tissue. As
81 epithelial cells are the first to come into contact with inhaled fibers, we investigated effects
82 of polyester and nylon microfibers on lung epithelial proliferation, differentiation, and

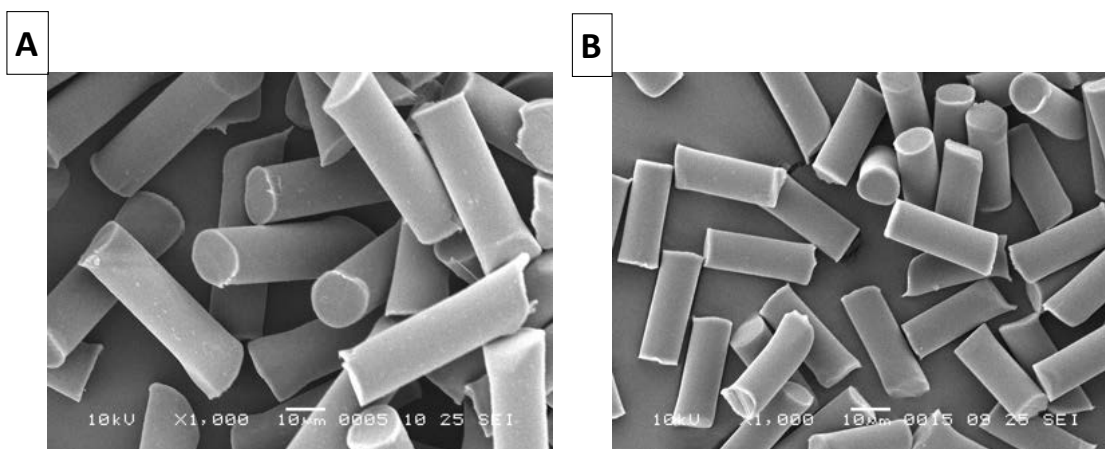
83 repair processes. For this we used lung organoids that are grown from primary lung
84 epithelial progenitor cells with support of a lung fibroblast cell line (32, 33). The epithelial
85 progenitors can develop into organoids consisting of alveolar epithelial cells or organoids
86 consisting of airway epithelial cells with help of growth factors produced by fibroblasts. We
87 found that in particular nylon microfibers negatively impacted developing airway
88 organoids, while developing alveolar organoids and already developed organoids of both
89 types appeared to be less affected. This negative effect was caused by still unknown
90 leachates from nylon that particularly inhibit differentiation of airway epithelial cells. We
91 therefore call for assessment of exposure levels in indoor environments and actual lung
92 deposition to accurately determine the risk of these fibers to human health.

93

94 Results

95 Characterization of reference microfibers

96 To produce reference textile fibers that resemble microplastics found in our indoor
97 environments, we used a method previous described by us to reproducibly generate fibers of
98 specific lengths (34). We particularly focused on polyester and nylon, because these are the
99 most abundant types of microplastics indoors (9, 35-38). As we spend the majority of our
00 time indoors, we may therefore be exposed most to these types of microplastics (39). Fibers
01 are commonly defined as having a length to diameter ratio of 3:1 (40). The fibers we
02 produced had a median size of 15x52 μm for polyester and 12x31 μm for nylon (Table S1).
03 Using scanning electron microscopy (SEM) we found these fibers to be rod-shaped with a
04 circular cross-section and had a smooth surface (Figure 1A and B). For our polyester fibers
05 energy dispersive X-ray (EDX) analysis confirmed the presence of carbon and oxygen
06 (Figure S1A). The recorded micro-Fourier transform infrared (μFTIR) spectrum showed
07 characteristic absorbance peaks of polyester (Figure S1B). The EDX spectrum for nylon
08 confirmed the presence of carbon, nitrogen and oxygen (Figure S1C) and the μFTIR
09 spectrum showed characteristic nylon absorbance peaks (Figure S1D).



10
11 **Figure 1. Morphology of reference microplastic fibers of standardized dimensions.**
12 *Representative SEM micrographs of (A) polyester microfibers (15x52 μm) and (B) nylon*
13 *microfibers (12x31 μm).*

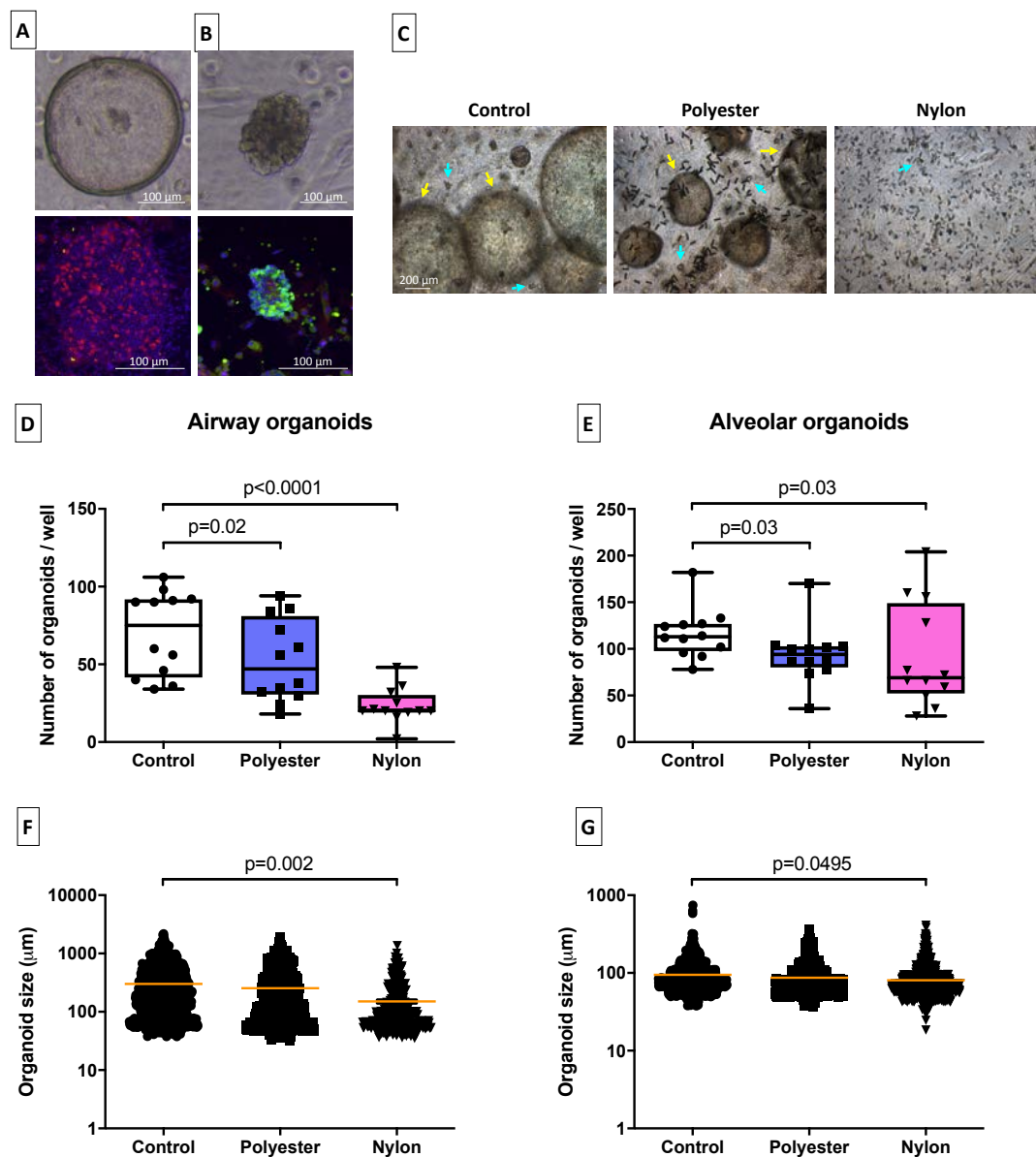
14
15

16 **Nylon microfibers inhibited growth of murine and human lung organoids**

17 Possible effects of microplastic fibers on lung epithelial proliferation, differentiation, and
18 repair processes were assessed *in vitro* using both murine and a human lung organoids.
19 Airways are lined with ciliated pseudostratified epithelium consisting of basal cells, ciliated
20 cells, and secretory cells like goblet cells and club cells, while alveoli consist of alveolar
21 epithelial cells type I and II (AECI and AECII). Basal cells and club cells have stem cell-
22 like abilities and basal cells can give rise to all important epithelial cells lining the airways,
23 while club cells can develop into ciliated cells, goblet cells, and AECII (41, 42). AECII can
24 behave as alveolar stem cells and can proliferate and develop into AECI (43). The lung
25 organoids we used in these studies self-assemble from the lung epithelial progenitor/stem
26 cells isolated from adult lung tissue, i.e. basal cells, club cells and AECII. The growth of
27 organoids from these progenitor cells is supported by proliferation and differentiation
28 enhancers produced by epithelial cells themselves and fibroblasts also present in our 3D
29 cultures (43).

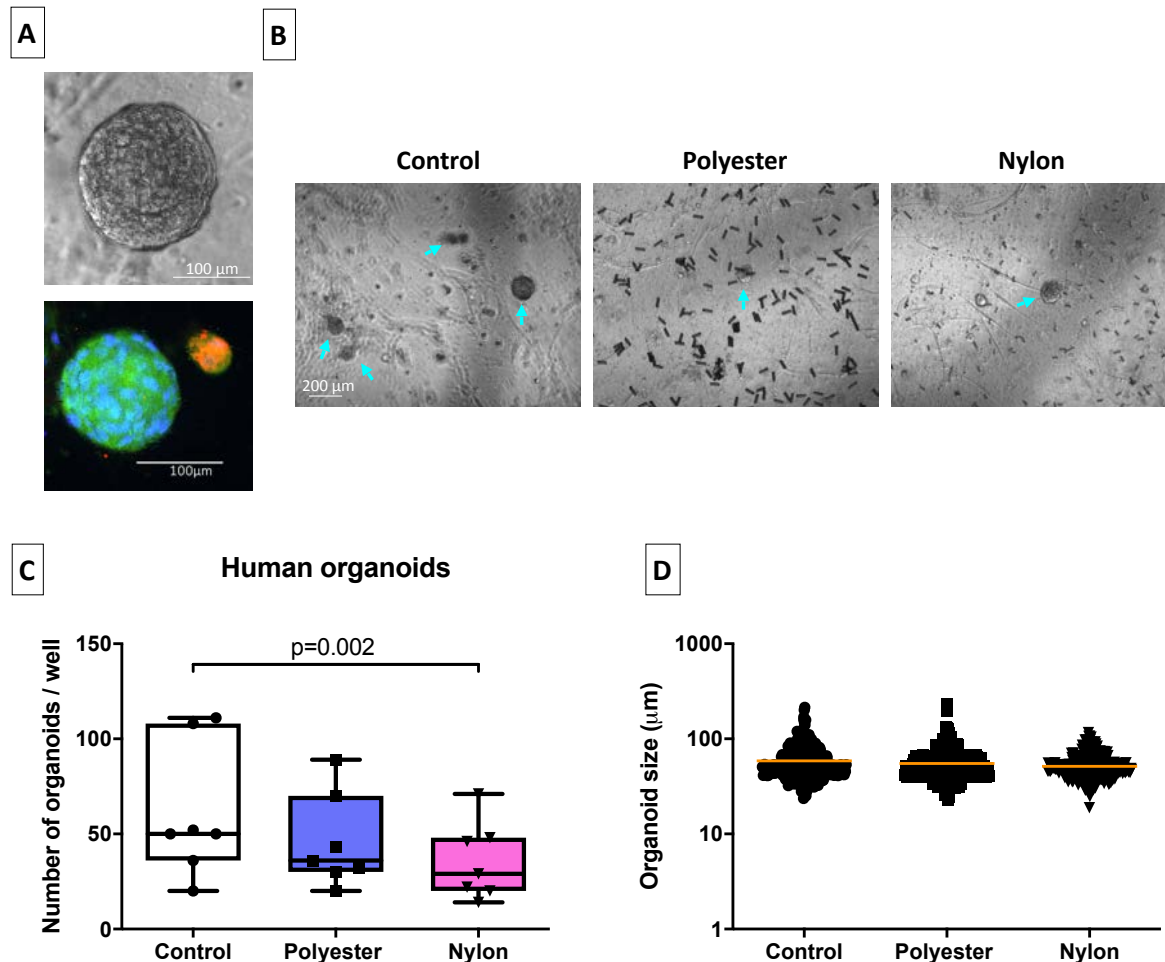
30 We first assessed the effects of several doses of fibers on organoid growth ranging from
31 2000-5000 fibers per well (Figure S2). The fibers were dispersed into liquid Matrigel at the
32 same time as the isolated epithelial cells and fibroblasts were added, after which the
33 Matrigel solidifies and epithelial progenitors start to form organoids. Based on these results
34 we continued with 5000 polyester or 5000 nylon fibers per well, equivalent to 122 $\mu\text{g/ml}$
35 polyester and 39 $\mu\text{g/ml}$ nylon, as this concentration had clear effects and was on the lower
36 end of the spectrum of concentrations used in other studies (7).

37 Murine lung organoids develop into two distinct phenotypes, i.e. acetylated α -tubulin-
38 positive airway organoids (Figure 2A) and prosurfactant protein C-positive alveolar
39 organoids (Figure 2B). We assessed the effects of the two types of fibers on these two
40 structures separately. Exposure during 14 days to either polyester or nylon microfibers
41 resulted in significantly fewer organoids (Figure 2C) compared to untreated controls (Figure
42 2D and E). The effect of nylon on airway organoids was most profound of the two types of
43 plastic and the two types of structures. Moreover, both airway and alveolar organoids were
44 significantly smaller in size following nylon microfiber exposure as compared to untreated
45 controls (Figure 2F and G).



46
 47 **Figure 2. Effects of microplastic fibers on growth of murine lung organoids.** Light
 48 microscopy images and fluorescence photographs of (A) acetylated α -tubulin-positive
 49 airway organoids (red) and (B) prosurfactant protein C-positive alveolar organoids
 50 (green). Nuclei were counterstained with DAPI (blue). (C) Representative light microscopy
 51 images of the different treatment conditions. Yellow arrows in the light microscopy images
 52 indicate airway organoids, whereas cyan arrows indicate alveolar organoids. (D and E)
 53 Quantification of the numbers and (F and G) quantification of the sizes of airway and
 54 alveolar lung organoids exposed for 14 days to no fibers, 5000 polyester, or 5000 nylon
 55 fibers (equivalent to 122 $\mu\text{g/ml}$ polyester or 39 $\mu\text{g/ml}$ polyester, $n=12$ independent
 56 isolations). Groups were compared using a Friedman test with Dunn's correction for
 57 multiple testing. $P<0.05$ was considered significant.

58 Similar results were observed in human lung organoids, that mainly develop into alveolar
59 organoids or mixed alveolar/airway organoids positive (Figure 3A). 14 day-exposure to
60 nylon microfibers resulted in significantly fewer human lung organoids (Figure 3B and C),
61 whereas the effects of polyester on organoid growth were less profound. The size of the
62 organoids was not affected by the presence of nylon microfibers (Figure 3D).



63 **Figure 3. Influence of microplastic fibers on growth of human lung organoids.** (A) The
64 morphology of the alveolar prosurfactant protein C-positive organoids (green) and mixed
65 acetylated α -tubulin/prosulfactant protein C-positive organoids (orange) as shown by light
66 and fluorescence microscopy. Nuclei were counterstained with DAPI (blue). (B)
67 Representative light microscopy images of all treatment conditions. Cyan arrows indicate
68 lung organoids. (C) Quantification of the numbers and (D) sizes of human lung organoids
69 following 14-day exposure to either no microfibers, 5000 polyester, or 5000 nylon fibers
70 (equivalent to 122 $\mu\text{g/ml}$ polyester or 39 $\mu\text{g/ml}$ polyester, $n=7$ independent isolations).
71 Groups were compared using a Friedman test with Dunn's correction for multiple testing.
72 $P<0.05$ was considered significant.

Environmental microplastic fibers impaired lung organoid growth as well

Having observed these effects after exposure to reference microfibers, we next performed similar experiments using environmentally relevant polyester and nylon fibers on murine lung organoids. These were made from white polyester and nylon fabrics purchased in a local fabric store and cut to sizes approximating the reference fibers. First, we characterized morphology and chemical composition of these fibers. For polyester, we observed a more heterogeneous size distribution as compared to the reference fibers, with fibers having a median size of $17 \times 63 \mu\text{m}$ (Figure 4A, Table S2), but a comparable EDX and μFTIR spectrum (Figure S3A and B). The nylon fibers had a disk-shaped appearance but similar dimensions as the reference nylon fibers (median $57 \times 20 \mu\text{m}$, Table S2). The EDX analysis revealed the expected C, N and O peaks for nylon (Figure S3C) and the μFTIR spectrum showed characteristic nylon absorbance peaks (Figure S3D).

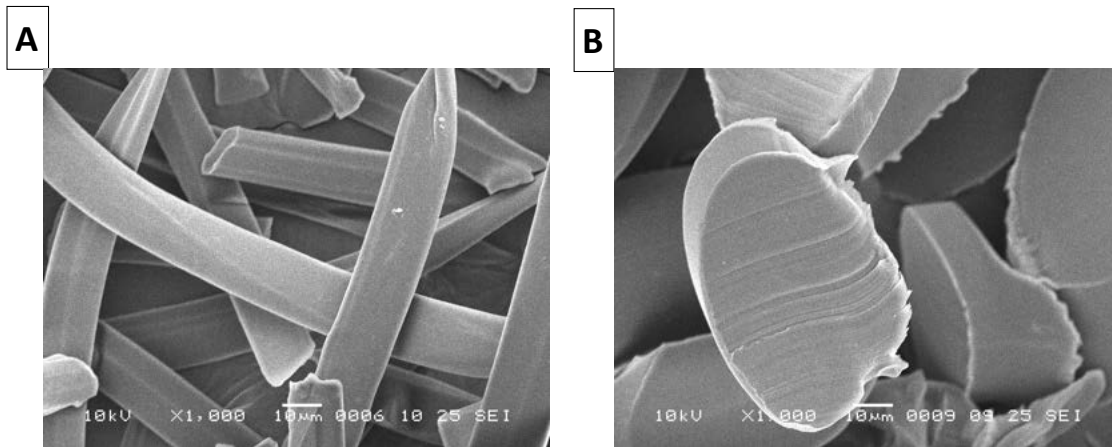
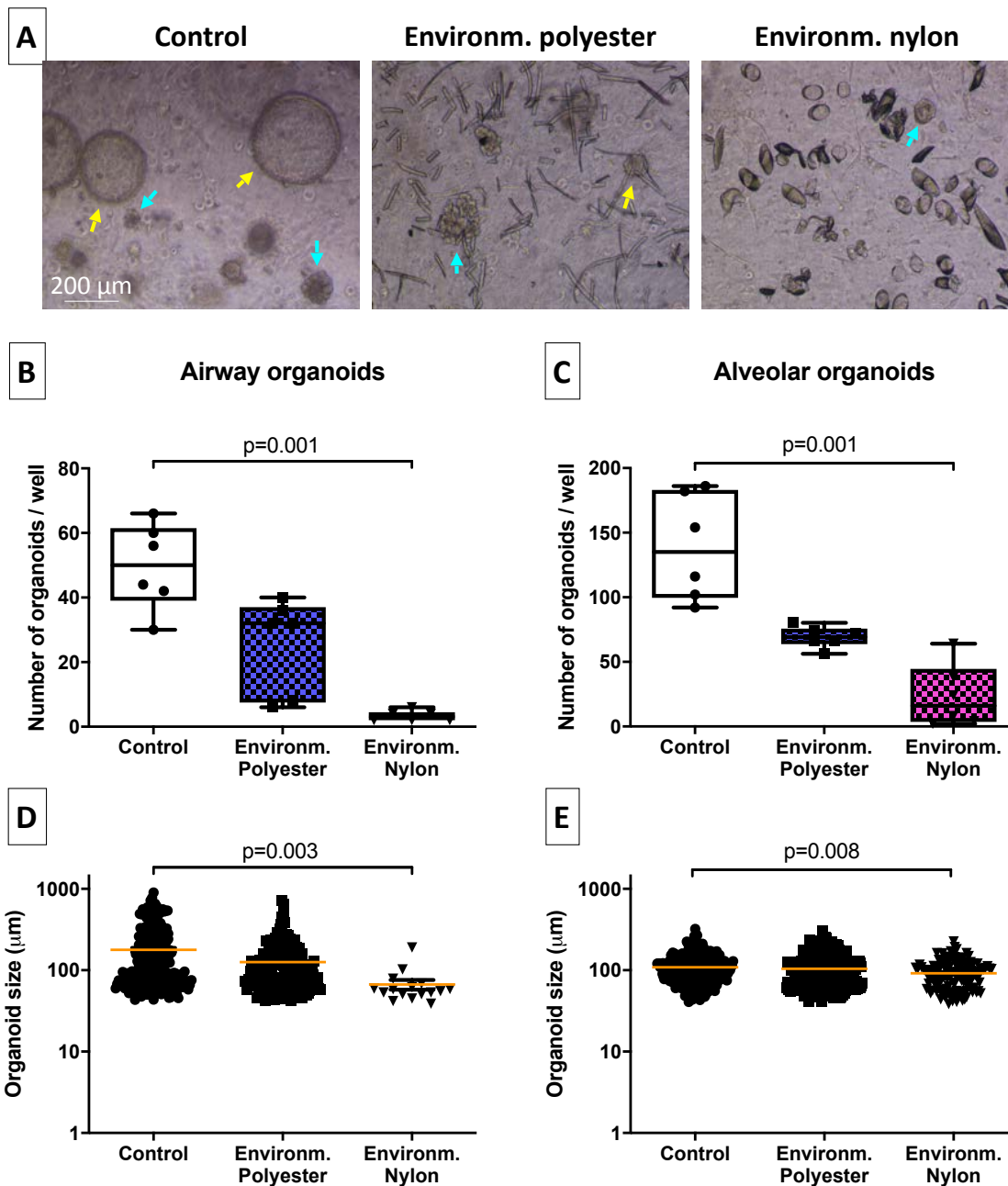


Figure 4. Morphology of environmental microplastic fibers. Representative SEM pictures of (A) polyester microfibrils ($17 \times 63 \mu\text{m}$) and (B) nylon microfibrils ($57 \times 20 \mu\text{m}$).

As observed with the reference fibers, exposure to environmental nylon microfibrils resulted in markedly fewer lung organoids (Figure 5A, B and C) as well as smaller organoids (Figure 5D and E).



92
93 **Figure 5: Effect of environmentally relevant textile fibers on growth of murine lung**
94 **organoids.** (A) Representative light microscopy images of all treatment conditions. Yellow
95 arrows in the light microscopy images indicate airway organoids, whereas cyan arrows
96 indicate alveolar organoids. (B and C) Quantification of the numbers and (D and E) sizes
97 of airway and alveolar organoids ($n=6$ independent isolations) following 14-day exposure
98 to either no microfibers, 5000 polyester or 5000 nylon microfibers (approximately
99 equivalent to 189 $\mu\text{g}/\text{ml}$ polyester or 531 $\mu\text{g}/\text{ml}$ nylon). Groups were compared using a
00 Friedman test with Dunn's correction for multiple testing. $P<0.05$ was considered
01 significant.

02 **Leaching nylon components caused a reduction in lung organoid growth**

03 Since organoid growth was most affected by nylon, both reference and environmentally
04 relevant fibers, we investigated whether this inhibition was caused by the physical presence
05 of fibers nearby the cells or by leaching components from these nylon fibers. Therefore, we
06 added nylon reference microfibers either on top of the Matrigel after it had set, thereby
07 preventing direct contact with the cells, or added leachate of these fibers to the medium
08 surrounding the Matrigel for 14 days. Interestingly, even when excluding physical contact
09 between the fibers and the cells or simply exposing the cells to medium with leachate, the
10 same effects on airway organoids were observed as when the forming organoids were
11 directly exposed to the fibers. We found significantly fewer airway organoids in the
12 presence of nylon microfibers on top of the gel or their leachate (Figure 6A and B)
13 compared to having the fibers inside the Matrigel. The number of alveolar organoids, on the
14 other hand, was unaffected (fibers on top) or even induced (leachate, Figure 6A and C)
15 compared to having the fibers inside the Matrigel. Additionally, the size of these airway
16 organoids was smaller as compared to untreated control organoids (Figure 6D), while only
17 slightly inhibiting the size of the alveolar organoids (Figure 6E). These data suggest that
18 specifically airway epithelial growth is inhibited by components leaching from nylon
19 microplastics.

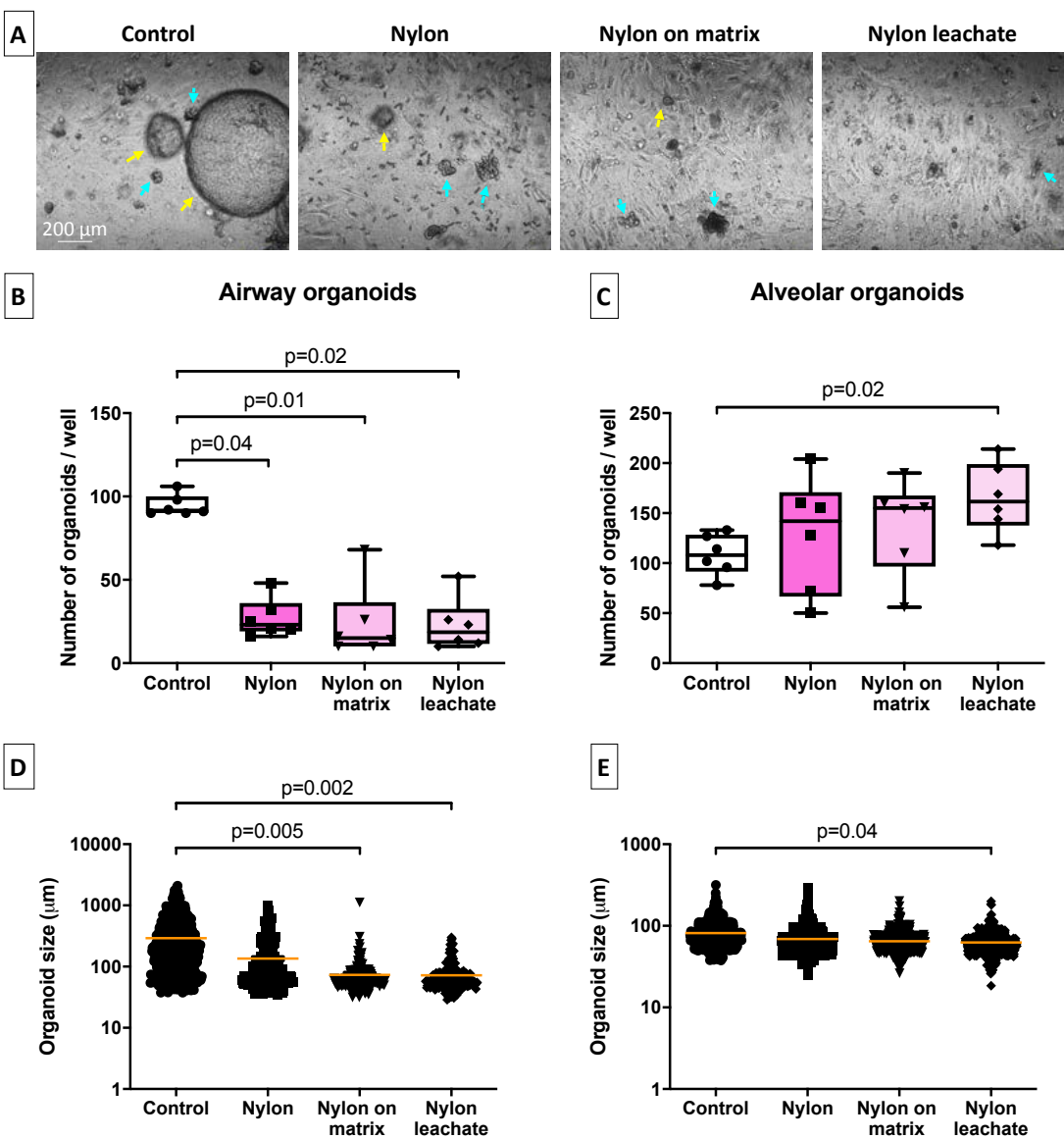


Figure 6. Impact of nylon reference microfibers and their leaching components on growth of murine lung organoids. (A) Representative light microscopy images of all treatment conditions. Yellow arrows in the light microscopy images indicate airway organoids, whereas cyan arrows indicate alveolar organoids. (B and C) Quantification of the numbers and (D and E) sizes of airway and alveolar organoids following either direct exposure to 5000 nylon microfibers or indirect exposure to nylon by adding 5000 microfibers (equivalent to 39 $\mu\text{g}/\text{ml}$ nylon) on top of the Matrigel or by adding nylon leachate to the culture medium ($n=6$ independent isolations). Groups were compared using a Friedman test with Dunn's correction for multiple testing. $P<0.05$ was considered significant.

32 The strong effects observed with the leachate suggested that some components and/or
33 degradation products may leak and/or form during fiber ageing at 37C. Thus in order to
34 determine the chemical identity of the components leaching from nylon reference
35 microfibers we used mass spectrometry analysis. This revealed high concentrations of
36 cyclic nylon oligomers (mono-, di- and trimers) in the leachate of nylon microfibers (Figure
37 S4A), which are known to develop as by-products during the production of nylon (44).
38 However, when exposing murine lung organoids to different concentrations of these
39 isolated oligomers separately or in combination, we observed no effects on either number or
40 size of organoids (Figure S4B-E showing the highest concentration that has been tested).
41 These data suggest that other components in nylon leachate are causing the inhibitory
42 effects on organoid growth. Recent work by Sait and Sørensen and colleagues showed that
43 the most abundant chemicals leaching from nylon are bisphenol A and benzophenone-3 (45,
44 46). However, we could not detect these in our leachate, suggesting that if they are present,
45 they are so in minute quantities. Initial experiments incubating organoids with different
46 concentrations of bisphenol A or benzophenone-3 did not show effects on organoid growth
47 of either of them suggesting they are indeed not the culprits in our leachate (data not
48 shown).

50 **Leaching nylon components mainly affected developing organoids**

51 As our experimental set-up specifically studied effects of microplastic fibers on developing
52 organoids, we next studied whether already-developed, mature organoids were also affected
53 by nylon microplastics. We therefore exposed organoids to nylon reference microfibers
54 during organoid formation as before (14-day incubation) and we additionally exposed fully
55 developed 14-day organoids to microfibers on top of the Matrigel or to nylon leachate for
56 an additional 7 days. Interestingly, in contrast to the strong effects observed on developing
57 organoids, we found that the compounds leaching from nylon had no effects on already-
58 developed organoids (Figure 7A), as reflected by unchanged numbers of organoids (Figure
59 7B and C) and unchanged sizes (Figure 7D and E). This suggests that these nylon leachates
60 are mostly harmful to differentiation of epithelial progenitors, but do not kill fully
61 differentiated epithelial cells.

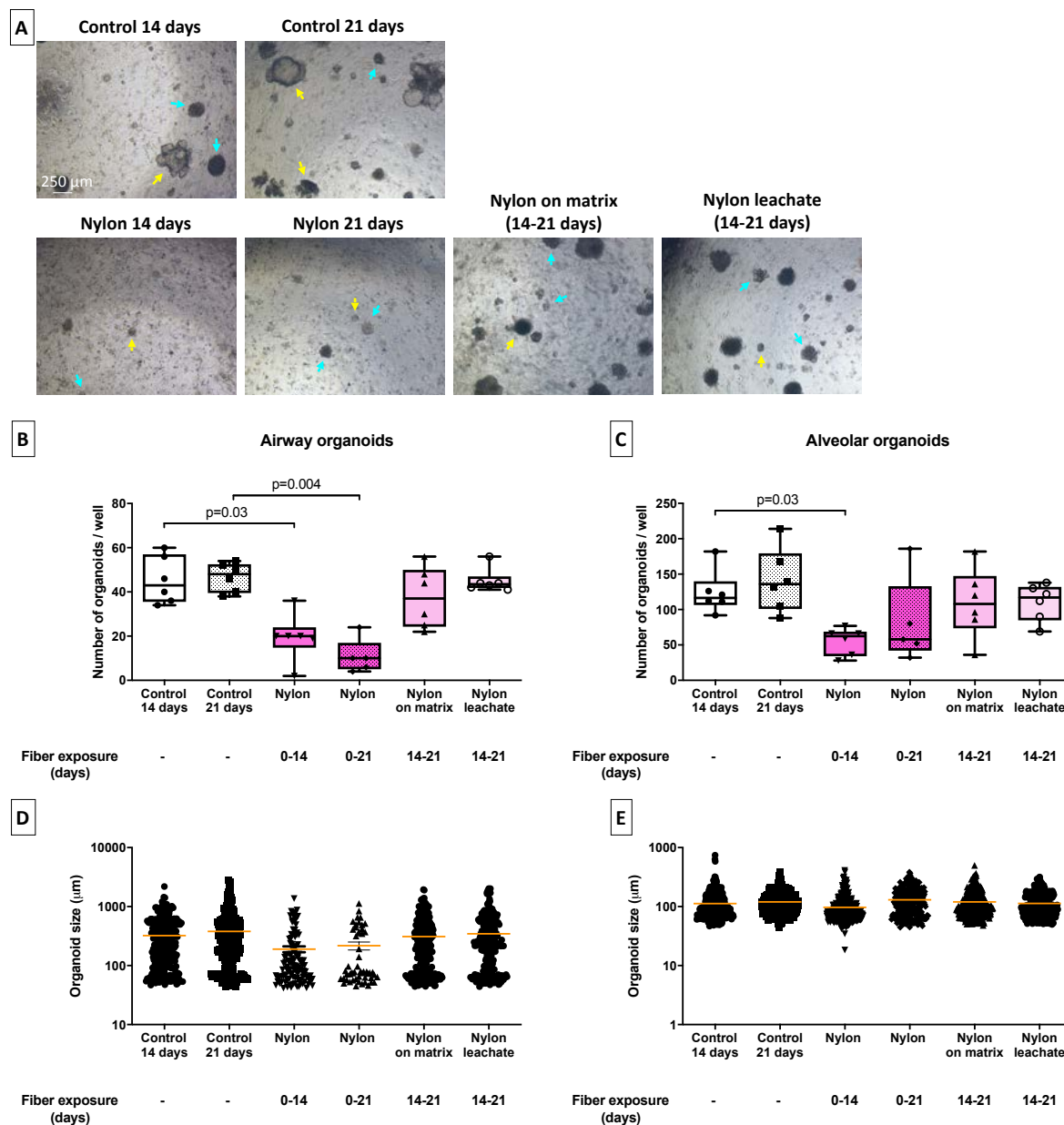


Figure 7. Effects of nylon reference fiber leachate on already-developed lung organoids.

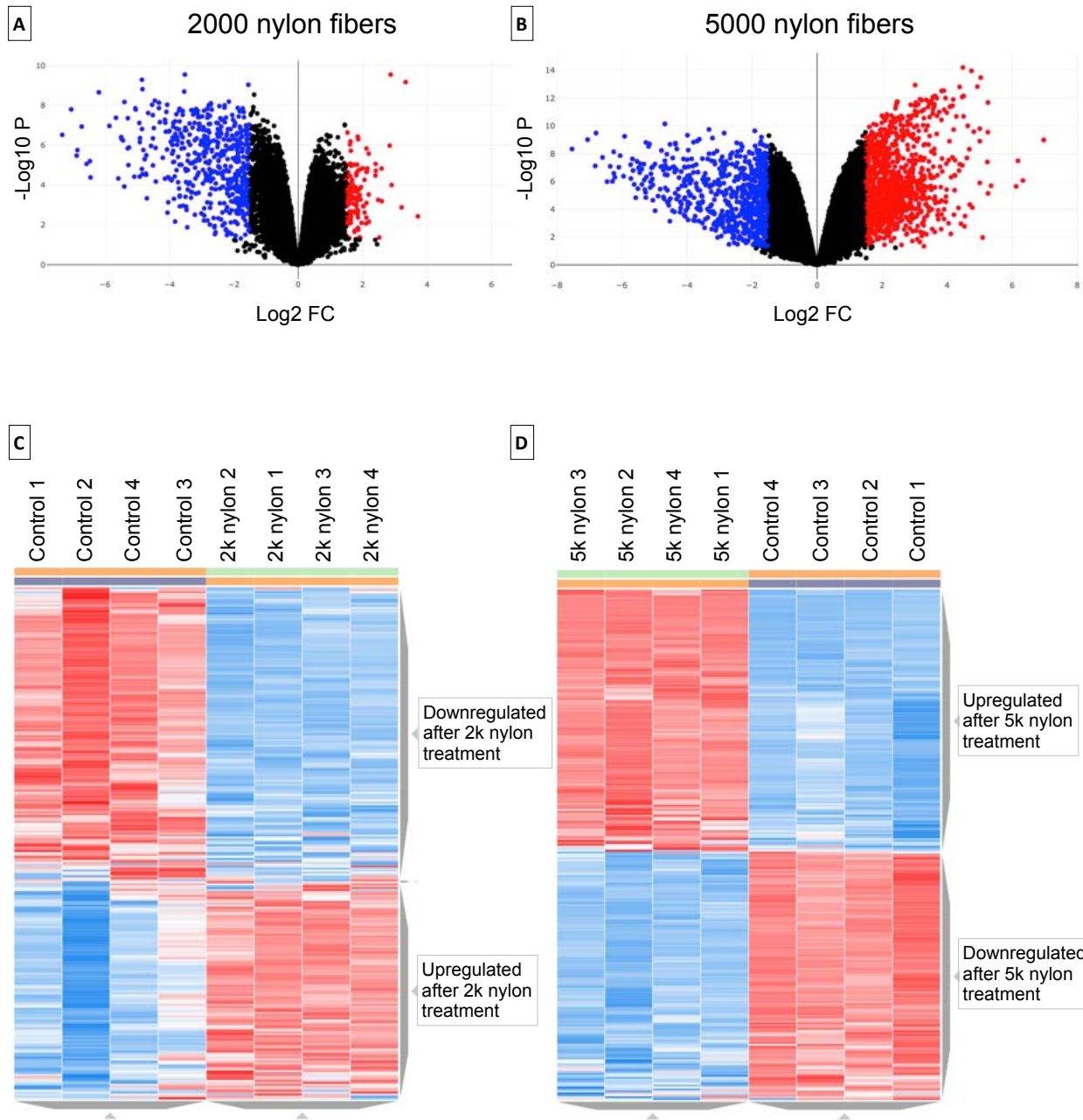
(A) Representative light microscopy images of all treatment conditions. Yellow arrows in the light microscopy images indicate airway organoids, whereas cyan arrows indicate alveolar organoids. (B and C) Quantification of the numbers and (D and E) sizes of airway and alveolar organoids following exposure to no or 5000 nylon microfibers (equivalent to 39 µg/ml nylon) for 14 or 21 days. A set of other organoids developed without treatment for 14 days and were exposed to nylon by adding 5000 microfibers (equivalent to 39 µg/ml nylon) on top of the Matrigel or by adding nylon leachate to the culture medium for another 7 days (n=6 independent isolations). Groups were compared using a Kruskal-Wallis test with Dunn's correction for multiple testing. $P < 0.05$ was considered significant.

74 **Exposure to nylon inhibited epithelial development pathways and stimulated** 75 **expression of ribosome components**

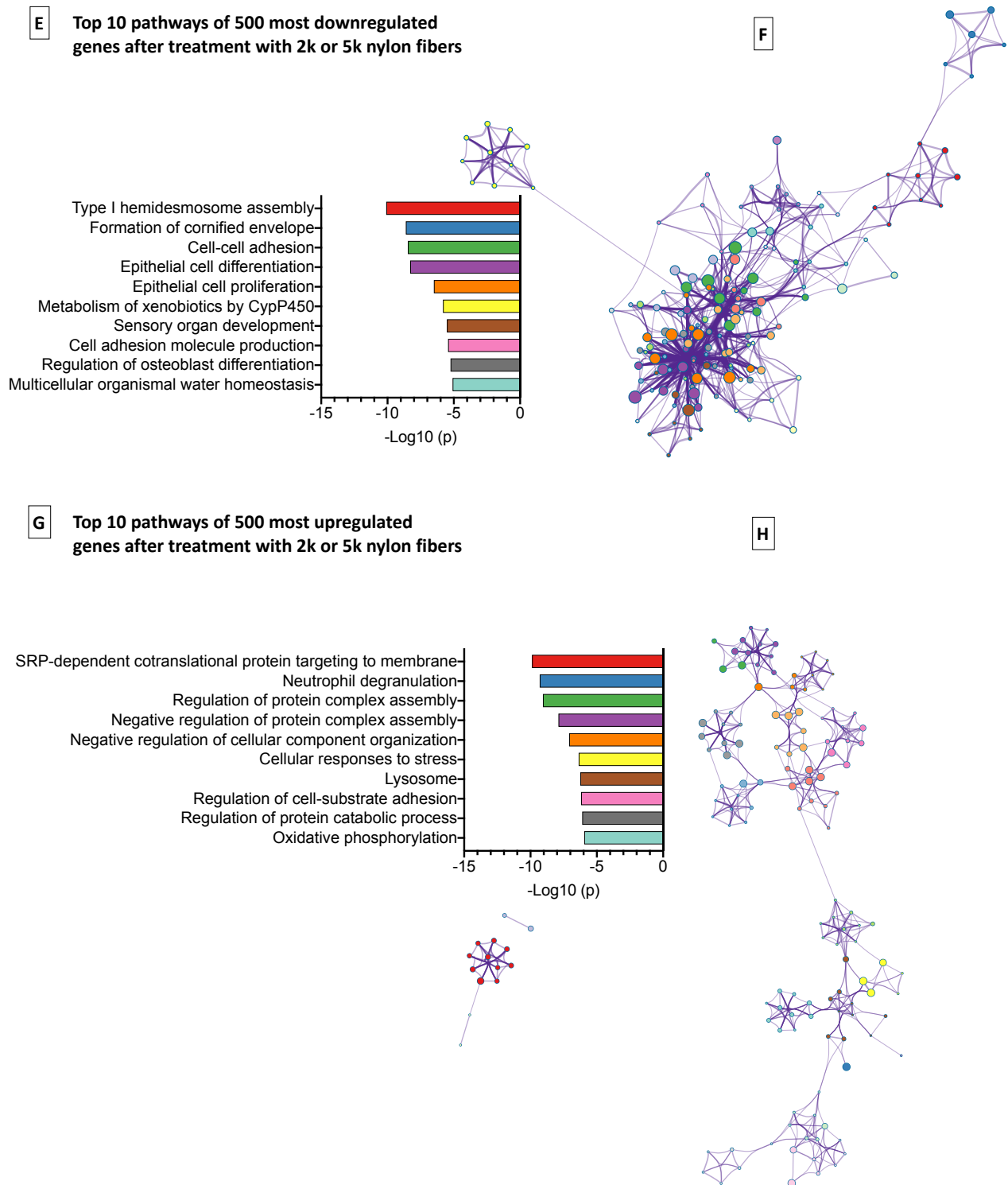
76 To better understand the mechanisms behind the observed effects on the growth of airway
77 organoids, we performed bulk RNA-sequencing (RNAseq) analysis on epithelial cells and
78 fibroblasts resorted from organoid cultures exposed to two different concentrations of nylon
79 fibers (2000 or 5000 fibers) or not. The condition of 2000 fibers was added because the
80 effect of 5000 fibers on airway epithelial development was already profound and we wanted
81 to investigate more subtle changes. However, both conditions had an enormous impact on
82 epithelial gene expression as depicted by the volcano plots (Figure 8A-D). Exposure to
83 2000 nylon fibers (equivalent to 16 $\mu\text{g/ml}$ nylon) resulted in 16455 transcripts being
84 differentially expressed at least two-fold compared to nonexposed controls, with an q value
85 <0.05 (p value corrected for the false discovery rate), with most being downregulated
86 (Figure 8A and C). Exposure to 5000 nylon fibers (equivalent to 39 $\mu\text{g/ml}$ nylon) resulted in
87 39395 transcripts being differentially expressed at least two-fold compared to nonexposed
88 controls, with most being upregulated (Figure 8B and D).

89 To reduce the number of transcripts, we then selected only those transcripts that had an
90 average basemean expression of at least 10 and were significantly (q value <0.05) up or
91 downregulated in both exposure conditions of 2000 and 5000 nylon fibers compared to
92 nonexposed controls. This resulted in 10764 transcripts that were differentially expressed
93 compared to nonexposed controls, with 5522 being downregulated and 5242 being
94 upregulated. The downregulated transcripts were then sorted on the lowest q value for
95 exposure to 2000 fibers and the upregulated transcripts were sorted on the lowest q value
96 for exposure to 5000 fibers and the top 500 genes of each were used for pathway analysis
97 using Metascape (47).

98 The top pathways identified for downregulated genes following nylon exposure were highly
99 enriched for epithelial development and function (figure 8E-F), while the top pathways
00 identified for upregulated genes were highly enriched for mRNA translation and protein
01 synthesis (figure 8G-H).



04



05
 06 **Figure 8: RNAseq analysis of epithelial cells exposed to nylon or not. (A)** Volcano plot of
 07 differentially expressed genes by epithelial cells exposed to 2000 nylon fibers (equivalent to
 08 16 $\mu\text{g/ml}$ nylon) or not. **(B)** Volcano plot of differentially expressed genes by epithelial cells
 09 exposed to 5000 nylon fibers (equivalent to 39 $\mu\text{g/ml}$ nylon) or not. Upregulated genes are
 10 marked in red, downregulated genes in blue. Genes were selected with thresholds of fold
 11 change >2 and $q < 0.05$. **(C)** Unsupervised clustering heat map of epithelial cells exposed to

12 2000 nylon fibers (equivalent to 16 $\mu\text{g/ml}$ nylon) or not. **(D)** Unsupervised clustering heat
13 map of epithelial cells exposed to 5000 nylon fibers (equivalent to 39 $\mu\text{g/ml}$ nylon) or not.
14 **(E)** Metascape bar graphs of top 10 nonredundant enrichment clusters of genes
15 downregulated by exposure to nylon ordered based on statistical significance (*p* value). **(F)**
16 Metascape enrichment network visualization showing the intra-cluster and inter-cluster
17 similarities of enriched terms of genes downregulated by exposure to nylon, up to ten terms
18 per cluster. Cluster annotations colors are shown in bar graph of panel E. **(G)** Metascape
19 bar graphs of top 10 nonredundant enrichment clusters of genes upregulated by exposure to
20 nylon ordered based on statistical significance (*p* value). **(H)** Metascape enrichment
21 network visualization showing the intra-cluster and inter-cluster similarities of enriched
22 terms of genes upregulated by exposure to nylon, up to ten terms per cluster. Cluster
23 annotations colors are shown in bar graph of panel E. 2k: 2000 fibers; 5k: 5000 fibers.

24
25 We then investigated expression of individual genes in the top 5 enriched pathways for up
26 and downregulated genes in more detail (Figures 8E-H). The top 5 enriched pathways for
27 downregulated genes were type I hemidesmosome assembly, formation of cornified
28 envelope, cell-cell adhesion, epithelial cell differentiation, and epithelial cell proliferation,
29 while the top 5 pathways for upregulated genes were SRP-dependent cotranslational protein
30 targeting to membrane, neutrophil degranulation, regulation of protein complex assembly,
31 negative regulation of protein complex assembly, and negative regulation of cellular
32 component organization.

33 We first investigated the downregulated genes and many of them represent important
34 epithelial populations in the lung. We therefore investigated genes associated with specific
35 epithelial populations (listed in table 1). The expression of these genes correlated well with
36 our organoid findings that airway epithelial cell growth was most affected by exposure to
37 nylon fibers, while alveolar epithelial cell growth was less affected (Figure 9). Both AEC I
38 and AEC II genes (Figure 9A) were only marginally lower expressed after exposure to
39 nylon while most genes for basal cells (Figure 9B), ciliated cells (Figure 9C), club cells and
40 goblet cells (Figure 9D) were expressed at significantly lower levels compared to controls
41 with two noticeable exceptions: ciliated cell marker *Tuba1a* and club cell marker *Scgb1a1*,
42 that were expressed at significantly higher levels compared to nonexposed controls.

43 Proliferation markers like proliferation marker protein 67 (*Mki67*), forkhead box protein M1
44 (*Foxm1*), and polo-like kinase 1 (*Plk1*, Figure 9E) confirmed this general lack of

45 proliferation in epithelial cells as all three were expressed at lower levels in a dose-
 46 dependent manner after exposure to nylon fibers. Expression of genes for signaling
 47 molecules essential for epithelial growth and development were impressively and dose-
 48 dependently downregulated by nylon exposure as well (Figure 9F), including *Notch1* and
 49 *Notch2* and their ligands Jagged 1 (*Jag1*) and 2 (*Jag2*) (48-50), *Bmp4* and *Bmp7* (51-53),
 50 *Wnt4* and *Wnt7a* (54, 55), and the receptor for hepatocyte growth factor, *Met*. The lower
 51 expression of basal cell-specific markers and essential factors that are needed for
 52 differentiation of other cell types like ciliated and goblet cells may explain why the growth
 53 of in particular airway organoids was inhibited most by nylon.

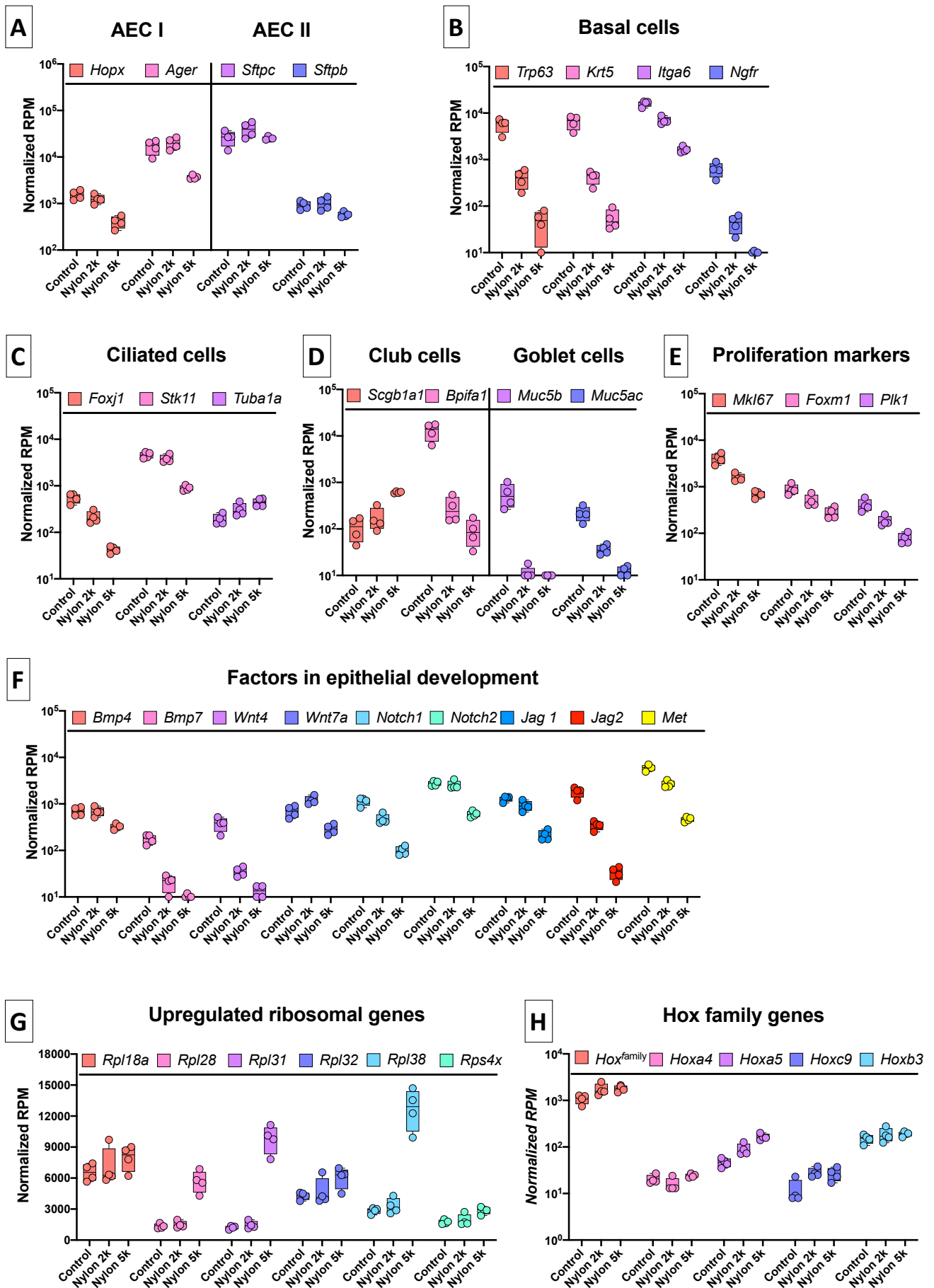
54
 55 **Table 1:** Markers associated with different epithelial populations in lung tissue.

Cell type	Protein name	Gene name
Epithelial cells present in airways		
Basal cells	Transformation-related protein 63	<i>Trp63</i>
	Keratin 5	<i>Krt5</i>
	Integrin alpha-6	<i>Itga6</i>
	Nerve growth factor receptor	<i>Ngfr</i>
Ciliated epithelial cells	Forkhead box J1	<i>Foxj1</i>
	Serine/threonine kinase 11	<i>Stk11</i>
	Acetylated alpha tubulin	<i>Tuba1a</i>
Goblet cells	Mucin 5 subtype B	<i>Muc5b</i>
	Mucin subtype AC	<i>Muc5ac</i>
Club cells	Secretoglobin family 1A member 1	<i>Scgb1a1</i>
	BPI fold containing family A member 1	<i>Bpifa1</i>
Epithelial cells present in alveoli		
Alveolar epithelial cells type I (AECI)	Homeodomain-only protein homeobox	<i>Hopx</i>
	Advanced glycosylation end-product specific receptor	<i>Ager</i>
Alveolar epithelial cells type II (AECII)	Surfactant protein C	<i>Sftpc</i>
	Surfactant protein B	<i>Sftpb</i>

56
 57 To exclude the possibility that these effects on epithelial cells were the result of a decreased
 58 support function from fibroblasts, for instance by nylon selectively killing fibroblasts or
 59 inhibiting the expression of important growth factors, we separately analyzed the resorted
 60 fibroblast fraction for expression of proliferation genes and important growth factors, i.e.
 61 *Mki67*, *Foxm1*, *Plk1*, fibroblast growth factors 2, 7, and 10 (*Fgf2*, *Fgf7*, and *Fgf10*), *Wnt2*,
 62 *Wnt5a*, and hepatocyte growth factor (*Hgf*) (33). None of these genes were negatively
 63 affected in fibroblasts after exposure to nylon fibers compared to untreated controls and
 64 expression of most actually went up slightly (Figure S5).

65 The genes most prominently upregulated after exposure to nylon fibers were mostly
66 encoding for ribosomal proteins, with ribosomal protein L28 (*Rpl28*), L31 (*Rpl31*), and L38
67 (*Rpl38*) being most profoundly upregulated (Figure 9G). Ribosomal proteins are a large
68 family of proteins and essential parts of ribosomes translating mRNA to protein. Recent
69 data has shown that heterogeneity in ribosomal protein composition within ribosomes
70 makes them selective for translating subpools of transcripts (56). For instance, Rpl38 has
71 been shown to regulate translation of the homeobox (*Hox*) genes, that are key in anatomical
72 development (57). We therefore also investigated the expression of all *Hox* genes and some
73 specific members of this family involved in lung epithelial development in more detail
74 (Figure 9H) (58, 59). After exposure to nylon fibers, expression of *Hox* family members
75 was significantly higher and this pattern was seen for highlighted members *Hoxa4*, *Hoxa5*,
76 *Hoxc9*, and *Hoxb3* as well.

65
66
67
68
69
70
71
72
73
74
75
76
77



79 **Figure 9: Expression profiles of individual genes from the pathway analyses.** Genes
80 shown were significantly differentially expressed in epithelial cells isolated from organoids
81 exposed to 2000 (2k) or 5000 (5k) nylon fibers compared to untreated controls according to
82 a false discovery rate of $q < 0.05$ ($n=4$ independent isolations). The following genes in the
83 following conditions were not significantly different: 2k nylon: *Hopx*, *Ager*, *Sftpc*, *Sftpb*,
84 *Stk11*, *Scgb1a1*, *Bmp4*, *Notch2*, *Hoxa4*; 5k nylon: *Hopx*, *Ager*, *Plk1*.
85 (A) Genes highly expressed by alveolar epithelial cells type I (AECI) and type II (AECII).
86 (B) Genes highly expressed in basal cells. (C) Genes highly expressed in ciliated cells. (D)
87 Genes highly expressed in club cells and goblet cells. (E) Genes associated with
88 proliferation. (F) Genes encoding factors important for epithelial development. (G) Genes
89 encoding ribosomal proteins. (H) Genes encoding Hox family genes.

92 Discussion

93 Recent reports have shown that man-made fibers are ubiquitously present in indoor air (9,
94 35-38). It is estimated that approximately 30% of those indoor fibers are of plastic origin,
95 particularly from textiles (9, 35-38). The lungs are continuously exposed to this airborne
96 microplastic pollution (60), but the consequences of common household exposure on our
97 lungs are unclear. In our present work, we found that both polyester and nylon microfibers
98 negatively affected the growth and development of human and murine lung organoids, with
99 nylon being the most harmful. Already established lung organoids were not affected and
00 therefore our results may be of particular importance for young children with developing
01 airways and for people undergoing high levels of epithelial repair, such as people with
02 respiratory diseases.

03
04 Nylon was found to be the most consistently harmful for growth of airway organoids and
05 was less inhibitory for growth of alveolar organoids, while polyester affected both types
06 equally but less profoundly than nylon. This was the case for our reference fibers as well as
07 environmentally relevant fibers made from fabrics purchased in a local fabric store. The
08 gene expression analysis also confirmed that growth of alveolar organoids was affected less
09 by nylon exposure and even appeared *induced* after treatment with leachate or lower
10 numbers of nylon fibers. The explanation for this finding may be found in the
11 downregulation of Notch signaling pathway members by nylon fibers. Multiple studies have

12 shown that Notch signaling is required for development of airway epithelial cells, most
13 specifically goblet cells, whereas disruption of this signaling boosts alveolar epithelial
14 development (61, 62). Both *Notch1* and *Notch2*, as well as their ligands *Jag1* and *Jag2* were
15 expressed at significantly lower levels after nylon treatment, suggesting disruption of Notch
16 signaling may be responsible for the divergent effect nylon has on airway versus alveolar
17 epithelial growth.

18 The Notch pathway, incidentally, is also important for the development of club cells (63).
19 Morimoto and colleagues showed that *Notch2* was involved in the decision between club
20 cell or ciliated cell development. Interestingly, the gene expression data for club cells and
21 ciliated cells were somewhat ambiguous, with important markers for these cell types having
22 higher expression (*Scgb1a1* for club cells and *Tub1a1* for ciliated cells) and others having
23 lower expression (*Bpifal* for club cells and *Foxj1* and *Stk11* for ciliated cells) after nylon
24 exposure. This may suggest that the lower expression of *Notch2* may be hampering the cell
25 fate decision between club and ciliated cells in some way, resulting in improperly
26 differentiated cell types. In combination with the inhibited development of basal epithelial
27 cells and goblet cells, this altered airway epithelial differentiation may explain the
28 bronchiolitis found in nylon flock workers and rats exposed to nylon (64-66).

29
30 Our results demonstrated that the negative effect of nylon fibers on development of
31 particularly airway organoids was caused by components leaching from these fibers. As the
32 most abundant components in this leachate, the cyclic oligomers, were not responsible for
33 this effect, we used RNAseq analysis to look for signatures of other components. Although
34 we could not detect bisphenol A in our leachate, it is of interest to note that exposure of fruit
35 flies to bisphenol A specifically upregulated ribosome-associated genes (67), similar to
36 what we found in our study. The association of these *Rpl* genes with the *Hox* family genes is
37 of particular interest for lung epithelial development. *Rpl38* was one of the three most
38 upregulated *Rpl* genes by nylon and was shown to interact with a specific subset of *Hox*
39 genes including *Hoxa4*, *Hoxa5*, and *Hoxb3* (57). These have all been associated with
40 epithelial differentiation, with *Hoxa5* taking a center stage in goblet versus club cell
41 differentiation (58, 59). Boucherat and colleagues showed that loss of *Hoxa5* drove
42 epithelial differentiation towards goblet cell differentiation at the expense of club cell
43 differentiation and *Scgb1a1* expression (58). Remarkably, *Hoxa5* was expressed at
44 significantly higher levels in our dataset in a dose-dependent manner after exposure to

45 nylon and we also found a matching dose-dependent increase in *Scgbl1* and decrease in
46 *Muc5ac* and *Muc5b* expression. Taken together our data suggest that component (s) in
47 nylon leachate may be skewing differentiation of epithelial progenitors away from airway
48 epithelial cells possibly through changes in expression of *Hoxa5* and/or *Notch*. Which
49 components or combinations of components are responsible for these effects is still an open
50 question.

51
52 A strength of using lung organoids is the opportunity to directly translate murine findings to
53 human lung epithelial repair (32, 33, 43, 68, 69). Using cells isolated from human lungs we
54 have shown human epithelial cells respond similarly to polyester and nylon fibers,
55 demonstrating our results are relevant for human epithelial differentiation and growth too.
56 Despite this advantage, lung organoids are a relatively simple model of lung tissue and lack
57 the immune and endothelial compartment present *in vivo*. Especially having the immune
58 compartment present could alter how lung tissue responds to these microplastic fibers. For
59 example, innate immune cells like macrophages are also one of the first cells to come into
60 contact with microplastic fibers following inhalation and macrophages are known to
61 respond strongly to inhaled particles and fibers (70) and are also important for lung repair
62 (71). It is therefore recommended to include lung macrophages in lung organoid cultures in
63 future studies as was done before by Choi *et al.* (72). This way, a more comprehensive view
64 on the interaction between pivotal lung cells and microplastics can be obtained.

65
66 The implication of our results for the human population is of high relevance. It is important
67 to note that similar to the high occupational exposure in industry workers, the microplastic
68 fiber doses as used in our *in vitro* experiments are much higher than daily exposure for most
69 people. Previous studies estimated that a male person with light activity may inhale around
70 272 microplastic particles per day based on air sampling using a breathing thermal manikin
71 (60). The total surface of airway epithelial cells is 2471 cm² for human lungs (73), resulting
72 in 0.1 particle/cm². Our murine cultures had an average of 70 airway organoids with an
73 average size of 320 μm, resulting in a total surface of 0.2 cm² that was incubated with 5000
74 fibers or 25,000 fibers/cm². For our calculations we assumed these particles/fibers will get
75 trapped onto airway epithelial cells. Generally particles or fibers of sizes between 10 and
76 100 μm will deposit onto epithelial cells covering airway walls (40). Only fibers with a
77 diameter smaller than 3 μm have the ability to penetrate deep into the lungs and reach the

78 alveoli. Our fiber sizes were limited by the availability of polyester and nylon filaments of
79 standardized small diameters and therefore were not small enough for alveolar deposition.
80 However, airway trapping can still cause local harm as we found nylon fibers to inhibit
81 airway epithelial differentiation most. It will therefore be crucial to study in more detail
82 how many and what kind of fibers deposit in which regions of the lungs and what fraction
83 can still be cleared. In addition, we need to gather more information about exposure levels
84 in indoor environments to assess real-life inhalation levels. A limitation here is the detection
85 of microplastics, as smaller particles might escape current detection methods (10, 74).
86 Especially our finding that epithelial differentiation and repair mechanisms are affected
87 most by microplastics exposure, suggests airborne microplastics may be most harmful to
88 young children with developing airways and to people undergoing high levels of epithelial
89 repair. These could be people with a chronic lung disease or even healthy individuals
90 suffering from a seasonal respiratory virus infection.

91
92 In conclusion, with the ongoing and growing use of plastics, potential associated health
93 problems in the human population may also increase. The results of the present study
94 strongly encourage to look in more detail at both hazard of and exposure to microplastic
95 fibers, and outcomes of these experiments will be valuable to advise organizations such as
96 the World Health Organization and Science Advice for Policy by European Academies who
97 have recently stated that more research is urgently needed (30, 31). Importantly, future
98 research should focus on examining the presence and number of such fibers both in our
99 indoor environment and in human lung tissue, to better estimate the actual risk of these
00 fibers to human health.

01
02
03

04 **Materials and Methods**

05

06 **Production of microfibers and leachate**

07 *Reference microfibers and leachate*

08 Microfibers of standardized dimensions were produced as described before (34). In short,
09 polyester and nylon fibers (both Goodfellow, UK) with filament diameters of $14\pm 3.5\ \mu\text{m}$
10 and $10\pm 2.5\ \mu\text{m}$ respectively were aligned by wrapping them around a custom-made spool,
11 coated with a thin layer of cryo compound (KP-CryoCompound, VWR International B.V.,
12 PA, USA) and frozen. Aligned fibers were cut into similar length parts ($\sim 2\ \text{cm}$) using a
13 scalpel (Swann-Morton, UK) and moulded onto a compact block that was oriented
14 perpendicular to the base of a cryomicrotome (Microm HM 525, Thermo Fisher Scientific,
15 MA, USA). Microfibers were cut at lengths of $50\ \mu\text{m}$ for polyester and $30\ \mu\text{m}$ for nylon,
16 after which the fibers were thawed, washed with water through a $120\ \mu\text{m}$ filter (Merck
17 Millipore, MA, USA) to remove miscut fibers and contaminants, collected by vacuum
18 filtration using $8\ \mu\text{m}$ polycarbonate membrane filters (Sterlitech, WA, USA) and stored dry
19 at -20°C .

20 Nylon leachate was produced by incubation of nylon reference microfibers in phosphate
21 buffered saline (PBS) for 7 days at 37°C in the dark, followed by filtration using a $0.2\ \mu\text{m}$
22 syringe filter (GE Healthcare Life Sciences, UK). The leachate was stored at -20°C until
23 further use.

24 *Environmental microfibers*

25 Environmental polyester and nylon textile microfibers were prepared from commercially
26 available pure fabrics. White polyester fabric was washed at 40°C in a washing machine
27 (Samsung, South Korea) and dried in a tumble dryer (Whirlpool, MI, US). Fibers with an
28 estimated filament diameter of $15\ \mu\text{m}$ were collected on the filter of the tumble dryer and
29 subsequently frozen with cryo compound and sectioned into lengths of $50\ \mu\text{m}$ using a
30 cryomicrotome. White nylon fabric (estimated filament diameter of $40\ \mu\text{m}$) was cut into
31 small squares, stacked, frozen with cryo compound, and cut into lengths of $12\ \mu\text{m}$. All
32 microfibers were thawed, washed with water through a $120\ \mu\text{m}$ filter, collected by vacuum
33 filtration ($8\ \mu\text{m}$ filter) and finally stored at -20°C .

34

35 **Characterization of microfibers and leachate**

36 *Scanning electron microscopy*

37 Samples were prepared for scanning electron microscopy (SEM) analysis on an aluminium
38 sample holder using adhesive carbon-coated tape. Excessive microfibers were removed
39 using pressurized air, after which the samples were sputter-coated with 10 nm of gold.
40 Images were obtained using a JSM-6460 microscope (Jeol, Japan) at an acceleration voltage
41 of 10 kV.

42 *Dimensions*

43 Digital photomicrographs were captured at 200× magnification using a Nikon Eclipse
44 TS100 inverted microscope coupled to a Nikon Digital Sight DS-U3 microscope camera
45 controller (both Japan), after which microfiber diameters and lengths (median of 200) were
46 determined using NIS-Elements AR 4.00.03 software.

48 **Ethics**

49 *Animal experiments*

50 The experimental protocol for the use of mice for epithelial cell isolations was approved by
51 the Animal Ethical Committee of the University of Groningen (The Netherlands) and all
52 experiments were performed according to strict governmental and international guidelines
53 on animal experimentation. C57BL/6 mice (8-14 weeks) were bred at the Central Animal
54 Facility of the University Medical Center Groningen (UMCG) (IVD 15303-01-004).
55 Animals received ad libitum normal diet with a 12 h light/dark cycle.

56 *Human lung tissue*

57 Histologically normal lung tissue was anonymously donated by individuals with COPD
58 (n=6) or without COPD (n=1) undergoing surgery for lung cancer and not objecting to the
59 use of their tissue. COPD patients included ex- and current- smoking individuals with
60 GOLD stage I-IV disease (GOLD I=1, GOLD II=2, GOLD IV=3). Subjects with other lung
61 diseases such as asthma, cystic fibrosis, or interstitial lung diseases were excluded. The
62 study protocol was consistent with the Research Code of the University Medical Center
63 Groningen (UMCG) and Dutch national ethical and professional guidelines
64 (www.federa.org). Sections of lung tissue of each patient were stained with a standard
65 haematoxylin and eosin staining and checked for abnormalities by a lung pathologist.

Cell cultures

Mouse lung fibroblasts (CCL-206, ATCC, Wesel, Germany) or human lung fibroblasts (MRC5, ATCC, CCL-171) were cultured in 1:1 DMEM (Gibco, MD, USA) and Ham's F12 (Lonza, Switzerland) or Ham's F12 respectively, both supplemented with 10% heat inactivated fetal bovine serum (FBS, GE Healthcare Life Sciences), 100 U/ml penicillin and 100 µg/ml streptomycin, 2 mM L-glutamine and 2.5 µg/ml amphotericin B (all Gibco). Fibroblasts were cultured at 37°C under 5% CO₂ and humidified conditions. For use in organoid cultures, near-confluent cells were proliferation-inactivated by incubation with 10 µg/ml mitomycin C (Sigma-Aldrich, MO, USA) in cell culture medium for 2 hours, after which they were washed in PBS, and left in normal medium for at least 1 hour before trypsinizing and counting.

Lung epithelial cell isolation

Mouse lung epithelial cell isolation

Epithelial cells were isolated from lungs of mice using antibody-coupled magnetic beads (microbeads) as described before (32, 33, 68). In short, mice were sacrificed under anaesthesia, after which the lungs were flushed with 0.9% NaCl and instilled with 75 caseinolytic units/1.5 ml dispase (Corning, NY, USA). After 45 minutes of incubation at room temperature, the lobes (excluding trachea and extrapulmonary airways) were homogenized in DMEM containing 100 U/ml penicillin and 100 µg/ml streptomycin and 40 µg/ml DNase1 (PanReac AppliChem, Germany), washed in DMEM (containing penicillin, streptomycin and DNase1), and the digested tissue was passed through a 100 µm cell strainer. The suspension was incubated for 20 minutes at 4°C with anti-CD31 and anti-CD45 microbeads in MACS buffer and magnetically sorted using LS columns. The CD31⁻/CD45⁻ flow-through was incubated for 20 minutes at 4°C with anti-CD326 (EpCAM) microbeads in MACS buffer, after which purified epithelial lung cells were obtained by positive selection using LS columns. CD326-positive epithelial cells were resuspended in CCL206 fibroblast medium, counted and seeded into Matrigel immediately after isolation with equal numbers of CCL206 fibroblasts, as described below. All materials were purchased at Miltenyi Biotec (Germany) unless stated otherwise.

97 *Human lung epithelial cell isolation*

98 Human lung epithelial cells were isolated from lung tissue specimens obtained from
99 patients. Peripheral lung tissue was minced and dissociated in DMEM-containing enzymes
00 (Multi Tissue Dissociation Kit) at 37°C using a gentleMACS Octo Dissociator. The cell
01 suspension was filtered (70 µm and 35 µm nylon strainer, respectively) prior to 20-minute
02 incubation at 4°C with anti-CD31 and anti-CD45 microbeads in MACS buffer. The
03 CD31⁻/CD45⁻ fraction was obtained by negative selection using an AutoMACS. Epithelial
04 cells were then isolated by positive selection after 20-minute incubation at 4°C with anti-
05 CD326 (EpCAM) microbeads in MACS buffer. Human EpCAM⁺ cells were resuspended
06 in 1:1 DMEM and Ham's F12, supplemented with 10% heat inactivated FBS, 100 U/ml
07 penicillin and 100 µg/ml streptomycin, 2 mM L-glutamine and 2.5 µg/ml amphotericin B,
08 counted and seeded into Matrigel immediately after isolation with equal numbers of MRC5
09 fibroblasts. All materials were purchased at Miltenyi Biotec unless stated otherwise.

11 **Lung organoid cultures**

12 Lung organoids were grown as previously described with minor modifications (32, 33, 68).
13 For mouse lung organoids, 10,000 EpCAM⁺ cells and 10,000 CCL206 fibroblasts were
14 seeded, and for human lung organoids, 5,000 EpCAM⁺ cells and 5,000 MRC5 fibroblasts
15 were seeded in 100 µl growth factor-reduced Matrigel matrix (Corning) diluted 1:1 in
16 DMEM:Ham's F-12 1:1 containing 10% FBS, 100 U/ml penicillin and 100 µg/ml
17 streptomycin, 2 mM L-glutamine and 2.5 µg/ml amphotericin B into transwell 24-well cell
18 culture plate inserts (Corning). Organoids were cultured in DMEM:Ham's F-12 1:1
19 supplemented with 5% FBS, 100 U/ml penicillin and 100 µg/ml streptomycin, 2 mM L-
20 glutamine, 2.5 µg/ml amphotericin B, 4 ml/l insulin-transferrin-selenium (Gibco), 25 µg/l
21 recombinant mouse (Sigma-Aldrich) or human epithelial growth factor (EGF, Gibco) and
22 300 µg/l bovine pituitary extract (Sigma-Aldrich). During the first 48h of culture, 10 µM Y-
23 27632 (Axon Medchem, the Netherlands) was added to the medium.

24 A titration curve for polyester or nylon microfibers was made with 2000, 3000, 4000 or
25 5000 fibers per well corresponding to approximately 49, 73, 98 and 122 µg/ml of polyester
26 fibers or 16, 23, 31, and 39 µg/ml of nylon fibers. For all other experiments, 5000 polyester
27 or nylon reference (equivalent to 122 µg/ml of polyester or 39 µg/ml of nylon) or
28 environmental microfibers (equivalent to 122 µg/ml of polyester or 39 µg/ml of nylon and)

29 were used per condition. Fibers were in direct contact with developing organoids during 14
30 days by mixing them with Matrigel and cells prior to seeding in the insert, except for those
31 experiments studying effects of leaching nylon components. In those cases, 5000 polyester
32 and nylon reference fibers were added on top of the organoids, thereby excluding physical
33 contact between the microfibers and the developing organoids, or equivalent amounts of
34 fiber leachate were added to the medium during 14 days of organoid culture. For testing the
35 effects of nylon oligomers, concentrations between 26.8 ng/ml and 53.6 µg/ml were used;
36 the latter concentration being twice as high as the used fiber concentrations (5000 fibers per
37 condition). Oligomers were synthesized and characterized as described in the
38 supplementary materials and methods. All organoid cultures were maintained for 14 to 21
39 days at 37 °C under 5% CO₂ and humidified conditions. Medium was refreshed 3 times per
40 week.

41 Organoid colony forming efficiency was quantified by manually counting the total number
42 of organoids per well after 14 or 21 days of culturing using a light microscope at 100×
43 magnification. For mouse organoids, a distinction was made between airway and alveolar
44 organoids, whereas for human organoids only one organoid phenotype was distinguished.
45 The diameter of the organoids was measured using a light microscope (Nikon, Eclipse Ti),
46 only including organoids larger than 50 µm in diameter, with a maximum of 50 organoids
47 per phenotype per well.

48

49 **Immunofluorescence staining**

50 Organoid cultures in Matrigel were washed with PBS, fixed in ice-cold 1:1 acetone and
51 methanol (both Biosolve Chimie, France) for 15 minutes at -20°C and washed again with
52 PBS after which aspecific antibody-binding was blocked for 2 hours in 5% bovine serum
53 albumin (BSA, Sigma-Aldrich). Organoids were incubated overnight at 4°C with the
54 primary antibodies (mouse anti-acetylated α -tubulin (Santa Cruz, TX, USA) and rabbit anti-
55 prosurfactant protein C (Merck, Germany)) both diluted 1:200 in 0.1% BSA and 0.1%
56 Triton (Sigma-Aldrich) in PBS. Next, after extensive but gentle washing with PBS,
57 organoids were incubated with the appropriate Alexa-conjugated secondary antibody for 2
58 hours at room temperature (Alexa Fluor 488 donkey anti rabbit IgG and Alexa Fluor 568
59 donkey anti mouse IgG, both Thermo Fisher Scientific) diluted 1:200 in 0.1% BSA and
60 0.1% Triton in PBS. Organoid cultures were washed with PBS, excised using a scalpel,
61 mounted on glass slides (Knittel, Germany) using mounting medium containing DAPI

(Sigma-Aldrich) and covered with a cover glass (VWR). Digital photomicrographs were captured at 200× magnification using a DM4000b fluorescence microscope and LAS V4.3 software (both Leica, Germany).

Isolation of epithelial cells and fibroblasts from organoid cultures

200,000 mouse EpCAM+ primary cells and 200,000 CCL206 fibroblasts (n=4 independent isolations) were seeded in 1 ml Matrigel diluted 1:1 in DMEM containing 10% FBS in 6-well plates (Greiner Bio-One, The Netherlands). 12.000 or 30.000 nylon reference microfibers were mixed with Matrigel and cells prior to seeding. Murine organoid culture medium was maintained on top and refreshed every two days. After 7 days, organoid cultures were digested with 50 caseinolytic units/ml dispase for 30 minutes at 37°C, transferred to 15 ml tubes, washed with MACS BSA stock solution and autoMACS rinsing solution (both Miltenyi), and digested further with trypsin (VWR) diluted 1:5 in PBS for 5 minutes at 37°C. The cell suspension was then incubated for 20 minutes at 4°C with anti-EpCAM microbeads in MACS buffer, after which the suspension was passed through LS columns. Both the EpCAM+ (epithelial cells) and EpCAM- (fibroblasts) cell fractions were used for RNA isolation and subsequent sequencing.

Library preparation and RNA sequencing

Total RNA was isolated from EpCAM+ and EpCAM- cell fractions using a Maxwell® LEV simply RNA Cells/Tissue kit (Promega, WI, USA) according to manufacturer's instructions. RNA concentrations were determined using a NanoDrop One spectrophotometer (Thermo Fisher Scientific). Total RNA (300 ng) was used for library preparation. Paired-end sequencing was performed using a NextSeq 500 machine (Illumina; mate 1 up to 74 cycles and mate 2 up to 9 cycles). Mate 1 contained the first STL (stochastic labeling) barcode, followed by the first bases of the sequenced fragments, and mate 2 only contained the second STL barcode. The generated data were subsequently demultiplexed using sample-specific barcodes and changed into fastq files using bcl2fastq (Illumina; version 1.8.4). The quality of the data was assessed using FastQC (75). The STL barcodes of the first mate were separated from the sequenced fragments using an in-house Perl script. Low quality bases and parts of adapter sequences were removed with Cutadapt (version 1.12; settings: q=15, O=5, e=0.1, m=36) (76). Sequenced poly A tails were

94 removed as well, by using a poly T sequence as adapter sequence (T (100); reverse
95 complement after sequencing). Reads shorter than 36 bases were discarded. The trimmed
96 fragment sequences were subsequently aligned to all known murine cDNA sequences using
97 HISAT2 (version 2.1.0; settings: k=1000, --norc). The number of reported alignments, k,
98 was given a high number in order to not miss any alignment results (some genes have up to
99 62 transcripts). Reads were only mapped to the forward strand (directional sequencing).
00 Fragment sequences that mapped to multiple genes were removed (unknown origin). When
01 fragments mapped to multiple transcripts from the same gene all but one were given a non-
02 primary alignment flag by HISAT2 (flag 256). These flags were removed (subtraction of
03 256) by the same Perl script in order to be able to use the Bash-based shell script
04 (dqRNASeq; see below) that is provided by Bioo Scientific (Perkin Elmer, MA, USA).
05 Fragments that mapped to multiple transcripts from the same gene were considered unique
06 and were counted for each of the transcripts. The number of unique fragments (or read
07 pairs) was determined for each transcript using the script provided by Bioo Scientific
08 (dqRNASeq; settings: s=8, q=0, m=1). Counts that were used for further analysis were
09 based on a unique combination of start and stop positions and barcodes (USS + STL). The
10 full data set is available as Supplemental Table S3 (Supplemental Material available online;
11 see <https://figshare.com/s/26a93797d19154dc418a>).

13 **Data analyses and statistics**

14 All statistics were performed with GraphPad Prism 9.0. Nonparametric testing was used to
15 compare groups in all experiments. For comparison of multiple-groups, a Kruskal wallis or
16 Friedman test was used for nonpaired or paired nonparametric data respectively with
17 Dunn's correction for multiple testing. Differences in organoid size between groups were
18 tested by using the average size of the organoids per independent experiment. Data are
19 presented as median \pm range and p-values <0.05 were considered significant.

20
21 For RNA sequencing data, the principal component analyses were performed in R using the
22 R package DESeq2 (version 1.26.0) (77) in order to visualize the overall effect of
23 experimental covariates as well as batch effects (function: plotPCA). Differential gene
24 expression analyses (treated vs. nontreated) was performed with the same R package
25 (default settings; Negative Binomial GLM fitting and Wald statistics; design=~condition),

26 following standard normalization procedures. Transcripts with differential expression >2
27 (nylon-treated versus nontreated fibroblasts or epithelial cells) and a false discovery rate
28 smaller than 0.05 (q value) were considered differentially expressed in that specific cell
29 type. Volcano plots and clustering heat maps were made using BioJupies (78). Pathway
30 analysis was done using Metascape (47).

33 References

- 35 1. J. Gasperi, S. L. Wright, R. Dris, F. Collard, C. Mandin, M. Guerrouache, V. Langlois, F.
36 J. Kelly, B. Tassin, Microplastics in air: Are we breathing it in. *Current Opinion in*
37 *Environmental Science & Health* **1**, 1-5 (2018).
- 38 2. C. M. Rochman, Microplastics research-from sink to source. *Science* **360**, 28-29 (2018).
- 39 3. I. E. Napper, A. Bakir, S. J. Rowland, R. C. Thompson, Characterisation, quantity and
40 sorptive properties of microplastics extracted from cosmetics. *Mar Pollut Bull* **99**, 178-185
41 (2015).
- 42 4. A. L. Andrady, Microplastics in the marine environment. *Mar Pollut Bull* **62**, 1596-1605
43 (2011).
- 44 5. V. Hidalgo-Ruz, L. Gutow, R. C. Thompson, M. Thiel, Microplastics in the marine
45 environment: a review of the methods used for identification and quantification. *Environ*
46 *Sci Technol* **46**, 3060-3075 (2012).
- 47 6. M. A. Browne, P. Crump, S. J. Niven, E. Teuten, A. Tonkin, T. Galloway, R. Thompson,
48 Accumulation of microplastic on shorelines worldwide: sources and sinks. *Environ Sci*
49 *Technol* **45**, 9175-9179 (2011).
- 50 7. J. C. Prata, J. P. da Costa, I. Lopes, A. C. Duarte, T. Rocha-Santos, Environmental
51 exposure to microplastics: An overview on possible human health effects. *Sci Total*
52 *Environ* **702**, 134455 (2020).
- 53 8. S. L. Wright, F. J. Kelly, Plastic and Human Health: A Micro Issue? *Environ Sci Technol*
54 **51**, 6634-6647 (2017).
- 55 9. R. Dris, J. Gasperi, C. Mirande, C. Mandin, M. Guerrouache, V. Langlois, B. Tassin, A
56 first overview of textile fibers, including microplastics, in indoor and outdoor
57 environments. *Environmental Pollution* **221**, 453-458 (2017).
- 58 10. R. Dris, J. Gasperi, M. Saad, C. Mirande, B. Tassin, Synthetic fibers in atmospheric
59 fallout: A source of microplastics in the environment? *Mar Pollut Bull* **104**, 290-293
60 (2016).
- 61 11. K. Donaldson, D. Brown, A. Clouter, R. Duffin, W. MacNee, L. Renwick, L. Tran, V.
62 Stone, The pulmonary toxicology of ultrafine particles. *J Aerosol Med* **15**, 213-220
63 (2002).
- 64 12. G. Oberdorster, E. Oberdorster, J. Oberdorster, Nanotoxicology: an emerging discipline
65 evolving from studies of ultrafine particles. *Environ Health Perspect* **113**, 823-839 (2005).
- 66 13. S. L. Wright, J. Ulke, A. Font, K. L. A. Chan, F. J. Kelly, Atmospheric microplastic
67 deposition in an urban environment and an evaluation of transport. *Environ Int* **136**,
68 105411 (2020).
- 69 14. J. Pauly, S. Stegmeier, H. Allaart, R. Cheney, P. Zhang, A. Mayer, R. Streck, Inhaled
70 cellulosic and plastic fibers found in human lung tissue. *Cancer Epidemiol Biomarkers*
71 *Prev* **7**, 419-428 (1998).

- 72 15. J. Burkhart, W. Jones, D. W. Porter, R. M. Washko, W. L. Eschenbacher, R. M. Castellan,
73 Hazardous occupational exposure and lung disease among nylon flock workers. *Am J Ind*
74 *Med Suppl* **1**, 145-146 (1999).
- 75 16. W. L. Eschenbacher, K. Kreiss, M. D. Lougheed, G. S. Pransky, B. Day, R. M. Castellan,
76 Nylon flock-associated interstitial lung disease. *Am J Respir Crit Care Med* **159**, 2003-
77 2008 (1999).
- 78 17. S. R. Goldyn, R. Condos, W. N. Rom, The burden of exposure-related diffuse lung
79 disease. *Semin Respir Crit Care Med* **29**, 591-602 (2008).
- 80 18. D. G. Kern, R. S. Crausman, K. T. Durand, A. Nayer, C. Kuhn, 3rd, Flock worker's lung:
81 chronic interstitial lung disease in the nylon flocking industry. *Ann Intern Med* **129**, 261-
82 272 (1998).
- 83 19. M. Shuchman, Secrecy in science: the flock worker's lung investigation. *Ann Intern Med*
84 **129**, 341-344 (1998).
- 85 20. S. E. Turcotte, A. Chee, R. Walsh, F. C. Grant, G. M. Liss, A. Boag, L. Forkert, P. W.
86 Munt, M. D. Lougheed, Flock worker's lung disease: natural history of cases and exposed
87 workers in Kingston, Ontario. *Chest* **143**, 1642-1648 (2013).
- 88 21. R. M. Washko, B. Day, J. E. Parker, R. M. Castellan, K. Kreiss, Epidemiologic
89 investigation of respiratory morbidity at a nylon flock plant. *Am J Ind Med* **38**, 628-638
90 (2000).
- 91 22. J. C. Pimentel, R. Avila, A. G. Lourenço, Respiratory disease caused by synthetic fibres: a
92 new occupational disease. *Thorax* **30**, 204-219 (1975).
- 93 23. E. M. Cordasco, S. L. Demeter, J. Kerkay, H. S. Van Ordstrand, E. V. Lucas, T. Chen, J.
94 A. Golish, Pulmonary manifestations of vinyl and polyvinyl chloride (interstitial lung
95 disease). Newer aspects. *Chest* **78**, 828-834 (1980).
- 96 24. P. J. Kole, A. J. Löhr, F. Van Belleghem, A. M. J. Ragas, Wear and Tear of Tyres: A
97 Stealthy Source of Microplastics in the Environment. *Int J Environ Res Public Health* **14**,
98 (2017).
- 99 25. C. E. Enyoh, A. W. Verla, E. N. Verla, F. C. Ibe, C. E. Amaobi, Airborne microplastics: a
00 review study on method for analysis, occurrence, movement and risks. *Environ Monit*
01 *Assess* **191**, 668 (2019).
- 02 26. L. F. Amato-Lourenço, L. Dos Santos Galvão, L. A. de Weger, P. S. Hiemstra, M. G.
03 Vijver, T. Mauad, An emerging class of air pollutants: Potential effects of microplastics to
04 respiratory human health? *Sci Total Environ* **749**, 141676 (2020).
- 05 27. G. Favarato, H. R. Anderson, R. Atkinson, G. Fuller, I. Mills, H. Walton, Traffic-related
06 pollution and asthma prevalence in children. Quantification of associations with nitrogen
07 dioxide. *Air Qual Atmos Health* **7**, 459-466 (2014).
- 08 28. M. Guarneri, J. R. Balmes, Outdoor air pollution and asthma. *Lancet* **383**, 1581-1592
09 (2014).
- 10 29. C. A. Keet, J. P. Keller, R. D. Peng, Long-Term Coarse Particulate Matter Exposure Is
11 Associated with Asthma among Children in Medicaid. *Am J Respir Crit Care Med* **197**,
12 737-746 (2018).
- 13 30. W. W. h. Organisation), *Microplastics in drinking-water* (World health Organisation,
14 Geneva, 2019), vol. CC BY-NC-SA 3.0 IGO.
- 15 31. S. A. f. P. b. E. A. SAPEA, *A scientific perspective on microplastics in nature and society*
16 (SAPEA, Berlin, 2019).
- 17 32. J. P. Ng-Blichfeldt, A. Schrik, R. K. Kortekaas, J. A. Noordhoek, I. H. Heijink, P. S.
18 Hiemstra, J. Stolk, M. Königshoff, R. Gosens, Retinoic acid signaling balances adult distal
19 lung epithelial progenitor cell growth and differentiation. *EBioMedicine*, (2018).
- 20 33. J. P. Ng-Blichfeldt, T. de Jong, R. K. Kortekaas, X. Wu, M. Lindner, V. Guryev, P. S.
21 Hiemstra, J. Stolk, M. Königshoff, R. Gosens, TGF- β activation impairs fibroblast ability

- 22 to support adult lung epithelial progenitor cell organoid formation. *Am J Physiol Lung*
23 *Cell Mol Physiol* **317**, L14-L28 (2019).
- 24 34. M. Cole, A novel method for preparing microplastic fibers. *Scientific Reports* **6**, (2016).
- 25 35. E. Gaston, M. Woo, C. Steele, S. Sukumaran, S. Anderson, Microplastics Differ Between
26 Indoor and Outdoor Air Masses: Insights from Multiple Microscopy Methodologies. *Appl*
27 *Spectrosc* **74**, 1079-1098 (2020).
- 28 36. S. O'Brien, E. D. Okoffo, J. W. O'Brien, F. Ribeiro, X. Wang, S. L. Wright, S.
29 Samanipour, C. Rauert, T. Y. A. Toapanta, R. Albarracin, K. V. Thomas, Airborne
30 emissions of microplastic fibres from domestic laundry dryers. *Sci Total Environ* **747**,
31 141175 (2020).
- 32 37. J. Zhang, L. Wang, K. Kannan, Microplastics in house dust from 12 countries and
33 associated human exposure. *Environ Int* **134**, 105314 (2020).
- 34 38. Q. Zhang, Y. Zhao, F. Du, H. Cai, G. Wang, H. Shi, Microplastic Fallout in Different
35 Indoor Environments. *Environ Sci Technol* **54**, 6530-6539 (2020).
- 36 39. B. L. Diffey, An overview analysis of the time people spend outdoors. *Br J Dermatol* **164**,
37 848-854 (2011).
- 38 40. TIMA (Thermal Insulation Manufacturers Association), *Man-made Vitreous Fibers:*
39 *Nomenclature, Chemical and Physical Properties* W. Eastes Ed (Nomenclature
40 Committee of Thermal Insulation Manufacturers' Association, Refractory Ceramic Fibers
41 Coalition (RCFC), Washington, DC, ed. 4th, 1993).
- 42 41. M. C. Basil, J. Katzen, A. E. Engler, M. Guo, M. J. Herriges, J. J. Kathiriya, R.
43 Windmueller, A. B. Ysasi, W. J. Zacharias, H. A. Chapman, D. N. Kotton, J. R. Rock, H.
44 W. Snoeck, G. Vunjak-Novakovic, J. A. Whitsett, E. E. Morrissey, The Cellular and
45 Physiological Basis for Lung Repair and Regeneration: Past, Present, and Future. *Cell*
46 *Stem Cell* **26**, 482-502 (2020).
- 47 42. B. Hogan, C. Barkauskas, H. Chapman, J. Epstein, R. Jain, C. Hsia, L. Niklason, E. Calle,
48 A. Le, S. Randell, J. Rock, M. Snitow, M. Krummel, B. Stripp, T. Vu, E. White, J.
49 Whitsett, E. Morrissey, Repair and regeneration of the respiratory system: complexity,
50 plasticity, and mechanisms of lung stem cell function. *Cell Stem Cell* **15**, 123-138 (2014).
- 51 43. C. E. Barkauskas, M. I. Chung, B. Fioret, X. Gao, H. Katsura, B. L. Hogan, Lung
52 organoids: current uses and future promise. *Development* **144**, 986-997 (2017).
- 53 44. Y. Abe, M. Mutsuga, H. Ohno, Y. Kawamura, H. Akiyama, Isolation and Quantification
54 of Polyamide Cyclic Oligomers in Kitchen Utensils and Their Migration into Various
55 Food Simulants. *PLoS One* **11**, e0159547 (2016).
- 56 45. S. T. L. Sait, L. Sørensen, S. Kubowicz, K. Vike-Jonas, S. V. Gonzalez, A. G.
57 Asimakopoulos, A. M. Booth, Microplastic fibres from synthetic textiles: Environmental
58 degradation and additive chemical content. *Environ Pollut* **268**, 115745 (2021).
- 59 46. L. Sørensen, A. S. Groven, I. A. Hovsbakken, O. Del Puerto, D. F. Krause, A. Sarno, A.
60 M. Booth, UV degradation of natural and synthetic microfibers causes fragmentation and
61 release of polymer degradation products and chemical additives. *Sci Total Environ* **755**,
62 143170 (2021).
- 63 47. Y. Zhou, B. Zhou, L. Pache, M. Chang, A. H. Khodabakhshi, O. Tanaseichuk, C. Benner,
64 S. K. Chanda, Metascape provides a biologist-oriented resource for the analysis of
65 systems-level datasets. *Nat Commun* **10**, 1523 (2019).
- 66 48. C. Di Sano, C. D'Anna, M. Ferraro, G. Chiappara, C. Sangiorgi, S. Di Vincenzo, A.
67 Bertani, P. Vitulo, A. Bruno, P. Dino, E. Pace, Impaired activation of Notch-1 signaling
68 hinders repair processes of bronchial epithelial cells exposed to cigarette smoke. *Toxicol*
69 *Lett* **326**, 61-69 (2020).
- 70 49. Y. Xing, A. Li, Z. Borok, C. Li, P. Minoo, NOTCH1 is required for regeneration of Clara
71 cells during repair of airway injury. *Stem Cells* **30**, 946-955 (2012).

- 72 50. D. Lafkas, A. Shelton, C. Chiu, G. de Leon Boenig, Y. Chen, S. S. Stawicki, C. Siltanen,
73 M. Reichelt, M. Zhou, X. Wu, J. Eastham-Anderson, H. Moore, M. Roose-Girma, Y.
74 Chinn, J. Q. Hang, S. Warming, J. Egen, W. P. Lee, C. Austin, Y. Wu, J. Payandeh, J. B.
75 Lowe, C. W. Siebel, Therapeutic antibodies reveal Notch control of transdifferentiation in
76 the adult lung. *Nature* **528**, 127-131 (2015).
- 77 51. A. Sountoulidis, A. Stavropoulos, S. Giaglis, E. Apostolou, R. Monteiro, S. M. Chuva de
78 Sousa Lopes, H. Chen, B. R. Stripp, C. Mummery, E. Andreakos, P. Sideras, Activation of
79 the canonical bone morphogenetic protein (BMP) pathway during lung morphogenesis
80 and adult lung tissue repair. *PLoS One* **7**, e41460 (2012).
- 81 52. C. Dean, M. Ito, H. P. Makarenkova, S. C. Faber, R. A. Lang, Bmp7 regulates branching
82 morphogenesis of the lacrimal gland by promoting mesenchymal proliferation and
83 condensation. *Development* **131**, 4155-4165 (2004).
- 84 53. Q. Tan, X. Y. Ma, W. Liu, J. A. Meridew, D. L. Jones, A. J. Haak, D. Sicard, G. Ligresti,
85 D. J. Tschumperlin, Nascent Lung Organoids Reveal Epithelium- and Bone
86 Morphogenetic Protein-mediated Suppression of Fibroblast Activation. *Am J Respir Cell*
87 *Mol Biol* **61**, 607-619 (2019).
- 88 54. A. Caprioli, A. Villasenor, L. A. Wylie, C. Braitsch, L. Marty-Santos, D. Barry, C. M.
89 Karner, S. Fu, S. M. Meadows, T. J. Carroll, O. Cleaver, Wnt4 is essential to normal
90 mammalian lung development. *Dev Biol* **406**, 222-234 (2015).
- 91 55. E. M. M. Abdelwahab, J. Rapp, D. Feller, V. Csongei, S. Pal, D. Bartis, D. R. Thickett, J.
92 E. Pongracz, Wnt signaling regulates trans-differentiation of stem cell like type 2 alveolar
93 epithelial cells to type 1 epithelial cells. *Respir Res* **20**, 204 (2019).
- 94 56. N. R. Genuth, M. Barna, The Discovery of Ribosome Heterogeneity and Its Implications
95 for Gene Regulation and Organismal Life. *Mol Cell* **71**, 364-374 (2018).
- 96 57. N. Kondrashov, A. Pusic, C. R. Stumpf, K. Shimizu, A. C. Hsieh, J. Ishijima, T. Shiroishi,
97 M. Barna, Ribosome-mediated specificity in Hox mRNA translation and vertebrate tissue
98 patterning. *Cell* **145**, 383-397 (2011).
- 99 58. O. Boucherat, J. Chakir, L. Jeannotte, The loss of Hoxa5 function promotes Notch-
00 dependent goblet cell metaplasia in lung airways. *Biol Open* **1**, 677-691 (2012).
- 01 59. T. Yoshimi, N. Nakamura, S. Shimada, K. Iguchi, F. Hashimoto, K. Mochitate, Y.
02 Takahashi, T. Miura, Homeobox B3, FoxA1 and FoxA2 interactions in epithelial lung cell
03 differentiation of the multipotent M3E3/C3 cell line. *Eur J Cell Biol* **84**, 555-566 (2005).
- 04 60. A. Vianello, R. L. Jensen, L. Liu, J. Vollertsen, Simulating human exposure to indoor
05 airborne microplastics using a Breathing Thermal Manikin. *Sci Rep* **9**, 8670 (2019).
- 06 61. P. N. Tsao, F. Chen, K. I. Izvolsky, J. Walker, M. A. Kukuruzinska, J. Lu, W. V. Cardoso,
07 Gamma-secretase activation of notch signaling regulates the balance of proximal and
08 distal fates in progenitor cells of the developing lung. *J Biol Chem* **283**, 29532-29544
09 (2008).
- 10 62. J. S. Guseh, S. A. Bores, B. Z. Stanger, Q. Zhou, W. J. Anderson, D. A. Melton, J.
11 Rajagopal, Notch signaling promotes airway mucous metaplasia and inhibits alveolar
12 development. *Development* **136**, 1751-1759 (2009).
- 13 63. M. Morimoto, R. Nishinakamura, Y. Saga, R. Kopan, Different assemblies of Notch
14 receptors coordinate the distribution of the major bronchial Clara, ciliated and
15 neuroendocrine cells. *Development* **139**, 4365-4373 (2012).
- 16 64. M. Sauler, M. Gulati, Newly recognized occupational and environmental causes of
17 chronic terminal airways and parenchymal lung disease. *Clin Chest Med* **33**, 667-680
18 (2012).
- 19 65. D. W. Porter, V. Castranova, V. A. Robinson, A. F. Hubbs, R. R. Mercer, J. Scabilloni, T.
20 Goldsmith, D. Schwegler-Berry, L. Battelli, R. Washko, J. Burkhart, C. Piacitelli, M.
21 Whitmer, W. Jones, Acute inflammatory reaction in rats after intratracheal instillation of

- 22 material collected from a nylon flocking plant. *J Toxicol Environ Health A* **57**, 25-45
23 (1999).
- 24 66. D. B. Warheit, T. R. Webb, K. L. Reed, J. F. Hansen, G. L. Kennedy, Jr., Four-week
25 inhalation toxicity study in rats with nylon respirable fibers: rapid lung clearance.
26 *Toxicology* **192**, 189-210 (2003).
- 27 67. A. T. Branco, B. Lemos, High intake of dietary sugar enhances bisphenol A (BPA)
28 disruption and reveals ribosome-mediated pathways of toxicity. *Genetics* **197**, 147-157
29 (2014).
- 30 68. Y. Hu, J. P. Ng-Blichfeldt, C. Ota, C. Ciminieri, W. Ren, P. S. Hiemstra, J. Stolk, R.
31 Gosens, M. Königshoff, Wnt/ β -catenin signaling is critical for regenerative potential of
32 distal lung epithelial progenitor cells in homeostasis and emphysema. *Stem Cells* **38**,
33 1467-1478 (2020).
- 34 69. J. H. Lee, E. L. Rawlins, Developmental mechanisms and adult stem cells for therapeutic
35 lung regeneration. *Dev Biol* **433**, 166-176 (2018).
- 36 70. G. Oberdörster, Toxicokinetics and effects of fibrous and nonfibrous particles. *Inhal*
37 *Toxicol* **14**, 29-56 (2002).
- 38 71. L. Florez-Sampedro, S. Song, B. Melgert, The diversity of myeloid immune cells shaping
39 wound repair and fibrosis in the lung. *Regeneration (Oxf)* **5**, 3-25 (2018).
- 40 72. J. Choi, J. E. Park, G. Tsagkogeorga, M. Yanagita, B. K. Koo, N. Han, J. H. Lee,
41 Inflammatory Signals Induce AT2 Cell-Derived Damage-Associated Transient
42 Progenitors that Mediate Alveolar Regeneration. *Cell Stem Cell* **27**, 366-382.e367 (2020).
- 43 73. R. R. Mercer, M. L. Russell, V. L. Roggli, J. D. Crapo, Cell number and distribution in
44 human and rat airways. *Am J Respir Cell Mol Biol* **10**, 613-624 (1994).
- 45 74. A. Ragusa, A. Svelato, C. Santacroce, P. Catalano, V. Notarstefano, O. Carnevali, F. Papa,
46 M. C. A. Rongioletti, F. Baiocco, S. Draghi, E. D'Amore, D. Rinaldo, M. Matta, E.
47 Giorgini, Plasticenta: First evidence of microplastics in human placenta. *Environ Int* **146**,
48 106274 (2021).
- 49 75. S. Andrew. (2010).
- 50 76. M. Martin, Cutadapt removes adapter sequences from high-throughput sequencing reads.
51 *2011* **17**, 3 (2011).
- 52 77. M. I. Love, W. Huber, S. Anders, Moderated estimation of fold change and dispersion for
53 RNA-seq data with DESeq2. *Genome Biol* **15**, 550 (2014).
- 54 78. D. Torre, A. Lachmann, A. Ma'ayan, BioJupies: Automated Generation of Interactive
55 Notebooks for RNA-Seq Data Analysis in the Cloud. *Cell Syst* **7**, 556-561.e553 (2018).
- 56 79. P. Peets, I. Leito, J. Pelt, S. Vahur, Identification and classification of textile fibres using
57 ATR-FT-IR spectroscopy with chemometric methods. *Spectrochim Acta A Mol Biomol*
58 *Spectrosc* **173**, 175-181 (2017).
- 59
- 60

61 Acknowledgments

62 **General:** The authors thank Habibie (University of Groningen, Department of Molecular
63 Pharmacology) for his help with the human organoid experiments, Imco Sibum, Paul
64 Hagedoorn, and Anko Eissens (University of Groningen, Department of Pharmaceutical
65 Technology and Biopharmacy) for their assistance at the scanning electron microscope,
66 Andreas W. Ehlers (University of Amsterdam, Van 't Hoff Institute for Molecular
67 Sciences) for his assistance with the NMR spectroscopy, and Elena Höppener (TNO,

68 Department Environmental Modeling Sensing and Analysis) for the energy dispersive X-
69 ray and infrared spectroscopy analysis of the microfibers.

70
71 **Funding:** ZonMW is gratefully acknowledged for their financial support with
72 Microplastics and Health grant 458001013.

73
74 **Author contributions:**

75 FD: Study design, collection and assembly of data, data analysis and interpretation,
76 manuscript writing, critical reading and revision.

77 SS: Collection and assembly of data, data analysis and interpretation, critical reading and
78 revision.

79 GE: Collection and assembly of data, data analysis and interpretation, critical reading and
80 revision.

81 XW: Collection and assembly of data, data analysis and interpretation, critical reading and
82 revision.

83 IB: Collection and assembly of data, critical reading and revision.

84 DB: Collection and assembly of data, data analysis and interpretation, experimental
85 material support, critical reading and revision.

86 IK: Collection and assembly of data, data analysis and interpretation, experimental
87 material support, critical reading and revision.

88 DS: Collection and assembly of data, data analysis and interpretation, experimental
89 material support, critical reading and revision.

90 RW: Collection and assembly of data, data analysis and interpretation, experimental
91 material support, critical reading and revision.

92 MC: Collection and assembly of data, data analysis and interpretation, experimental
93 material support, critical reading and revision.

94 AS: Data analysis and interpretation, critical reading and revision.

95 RG: Data analysis and interpretation, study design, experimental material support, critical
96 reading and revision.

97 BM: Collection and assembly of data, study design, data analysis and interpretation,
98 financial support, manuscript writing, critical reading and revision.

99
00 **Competing interests:** The authors declare no competing interests.

01
02 **Data and materials availability:** All data needed to evaluate the conclusions in the paper are
03 present in the paper and/or the Supplementary Materials. Additional data related to this
04 paper may be requested from the authors.

08 **Supplementary Materials and methods**

09

10 **Energy dispersive X-ray spectroscopy**

11 Samples were prepared for energy dispersive X-ray (EDX) spectroscopy analysis on an
12 aluminium sample holder using adhesive carbon coated tape. Excessive microfibers were
13 removed using pressurized air, after which the samples were sputter coated with 10 nm of
14 carbon. The EDX measurements were performed with a Tescan MAIA III GMH field
15 emission scanning electron microscope (Czech Republic) equipped with a Bruker X-Flash
16 30 mm² silicon drift energy dispersive X-ray microanalysis detector (MA, USA).

17

18 **Micro-Fourier transform infrared spectroscopy**

19 Micro-Fourier transform infrared spectroscopy (μ FTIR) measurements were performed
20 using a Thermo Nicolet iN10 micro Fourier transform infrared microscope. Spectra were
21 recorded in the wavelength range from 4000 to 675 cm⁻¹ using a spectral resolution of 8
22 cm⁻¹. For the transmission measurements of the polyester reference material and the
23 polyester and nylon environmental fibers, a small amount of the microfibers was
24 transferred onto a diamond micro compression cell where the samples were compressed.
25 For the reflection measurements of the nylon reference material and the polyester and
26 nylon environmental fibers, a small portion of microfibers was suspended in water. The
27 suspension was subsequently filtered over a gold coated 0.8 μ m polycarbonate filter (TJ
28 Environmental, The Netherlands). A subset of approximately 100 fibers was individually
29 measured directly on the filter using the reflection mode of the μ -FTIR equipment.

30

31 **Extraction of nylon oligomers (mono-, di- and trimer)**

32 A round bottom flask containing 25.1 g cryogenically milled nylon powder (PA66, Sigma-
33 Aldrich) and 500 ml methanol (VWR) was equipped with a reflux condenser and the
34 suspension was stirred overnight at 50°C. Next, the suspension was cooled to
35 approximately 30°C and filtered over a cellulose filter (VWR) to remove the remaining
36 powder. The solvent was removed *in vacuo* using a rotary evaporator (Büchi rotavapor R-
37 215, Switzerland). A white solid was obtained (yield 220 mg), of which the composition
38 was determined using liquid chromatography/mass spectrometry (LC/MS) analysis.

39 Isolation of nylon oligomers (mono-, di- and trimer)

40 A column for silica gel chromatography (\varnothing 30 mm, VWR) was charged with silica gel 60
41 (27 g, 0.063-0.200 mm, Merck) and dichloromethane (DCM, VWR) as eluent. The crude
42 extract containing the mixture of oligomers (200 mg) was added on top of the silica gel
43 column and oligomers were separated on the column using DCM:methanol as eluent
44 (DCM:MeOH gradient: 100:0 \rightarrow 90:10 \rightarrow 80:20), which resulted in complete separation
45 of the oligomers. The collected fractions were checked for the presence of product using
46 LC/MS. The fractions containing pure oligomer were combined, filtered over a glass filter
47 (VWR) and subsequently the solvent was removed *in vacuo*. The obtained solids were
48 further dried *in vacuo*, after which the pure oligomers were obtained as white solids. The
49 structure of the oligomers was confirmed by ^1H NMR spectroscopy.

51 Liquid chromatography/mass spectrometry

52 *Qualitative analysis of nylon leachate and oligomers*

53 Qualitative analysis of nylon oligomers was performed with an Agilent 1260 series high-
54 performance liquid chromatographer (CA, USA) equipped with a 100 x 2 mm, 3 μm
55 Gemini NX-C18 110 Å LC Column (Phenomenex, Utrecht, The Netherlands), coupled
56 with an Agilent 6410 triple quadrupole LC/MS with electron spray ionization (ESI) in
57 positive SCAN mode. In addition, the LC/MS analysis of the nylon leachate was
58 performed with the Agilent 1260 liquid chromatographer coupled to an Agilent 6460 triple
59 quadrupole LC/MS with Jetstream ESI in positive SCAN mode. A sample volume of 5 μl
60 was injected with a column temperature of 60 $^{\circ}\text{C}$ and a flow rate of 200 $\mu\text{l min}^{-1}$. The
61 sample was eluted with a gradient of Milli-Q water (containing 5 mM ammonium formate
62 with 0.0025% formic acid (both Sigma-Aldrich), eluent A) and methanol (containing 5
63 mM ammonium formate with 0.0025% formic acid, eluent B) with a flow rate of 0.5 ml
64 min^{-1} . Eluent B was increased from 10% to 90% in 10 minutes and maintained for 3
65 minutes. After this, eluent B was decreased to 10% in 0.1 minute and maintained for 1.9
66 minute to complete the cycle of 15 minutes. Mass spectrometry was performed with a gas
67 temperature of 350 $^{\circ}\text{C}$ and a flow rate of 10 l min^{-1} . Stealth gas temperature (for Agilent
68 6460) was set at 400 $^{\circ}\text{C}$ with a flow rate of 12 l min^{-1} . The capillary voltage was set at
69 4000 V.

Direct injection of nylon leachate

An injection volume of 10 μ l diluted nylon leachate was directly injected into an Agilent 6410 triple quadrupole MS system with ESI in positive SCAN mode. The conditions were as follows: gas temperature 350 °C, flow rate 10 l min⁻¹, mobile phase 50:50 ratio of 80:20 acetonitrile (VWR):Milli-Q water with 5 mM ammonium formate and 10:90 acetonitrile:Milli-Q water with 5 mM ammonium formate, scan range 50–1000 Da, capillary voltage 3500 V.

¹H Nuclear magnetic resonance

The chemical structure of the oligomers was confirmed by ¹H NMR spectroscopy (Bruker Avance 400 spectrometer). The oligomers were dissolved in ~0.5 ml CD₃OD:CDCl₃ (1:1) (Sigma-Aldrich). The spectra were recorded at 24 °C, and internally referenced to the residual solvent resonance (CD₃OD: ¹H δ 3.31).

Nylon monomer, yield = 77 mg. ¹H NMR (400.1 MHz, CD₃OD/CDCl₃ 50:50, 297 K) δ = 7.56 (br. m, 2H; NHCO), 3.22 (m, 4H, NHCH₂), 2.19 (m, 4H, COCH₂), 1.63 (m, 4H, COCH₂CH₂), 1.54 (m, 4H, NHCH₂CH₂), 1.32 (m, 4H, NH (CH₂)₂CH₂).

Nylon dimer, yield = 74 mg. ¹H NMR (400.1 MHz, CD₃OD/CDCl₃ 50:50, 297 K) δ = 7.68 (br. m, 4H; NHCO), 3.15 (t, 8H, NHCH₂), 2.18 (m, 8H, COCH₂), 1.60 (m, 8H, COCH₂CH₂), 1.47 (m, 8H, NHCH₂CH₂), 1.31 (m, 8H, NH (CH₂)₂CH₂).

Nylon trimer, yield = 16 mg. ¹H NMR (400.1 MHz, CD₃OD/CDCl₃ 50:50, 297 K) δ = 7.74 (br. m, 6H; NHCO), 3.14 (t, 12H, NHCH₂), 2.18 (m, 12H, COCH₂), 1.60 (m, 12H, COCH₂CH₂), 1.48 (m, 12H, NHCH₂CH₂), 1.32 (m, 12H, NH (CH₂)₂CH₂).

95 **Supplementary tables and figures**

96

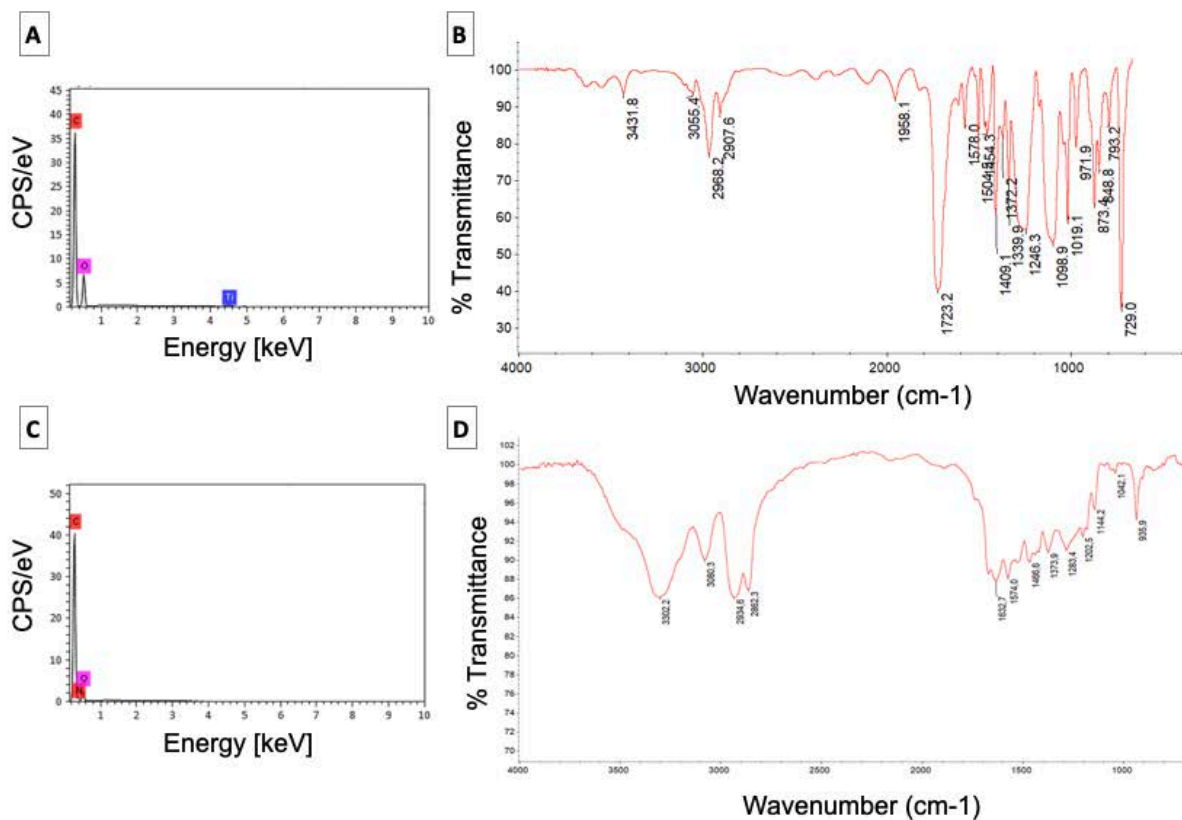
97 **Table S1.** Size characteristics of polyester and nylon reference microfibers.

	Microfiber size Diameter x length (μm)	
	Polyester	Nylon
25% percentile	14x50	11x29
Median	15x52	12x31
75% percentile	15x53	12x32
Minimum	13x22	9x24
Maximum	18x64	14x74

98

99

00



01

02 **Figure S1: Characterization of the reference microfibers using energy dispersive X-ray**
03 **- and infrared spectroscopy.** (A) EDX spectrum of polyester, confirming the presence of
04 carbon (C) and oxygen (O), and additionally revealing the presence of titanium (Ti),
05 which can be ascribed to small TiO₂ pigment particles used as filler material in these
06 fibers. (B) μFTIR spectrum of polyester with characteristic absorbance peaks (2968 cm⁻¹,
07 C-H stretch; 1723 cm⁻¹, C=O stretch; 1246 cm⁻¹, C-O stretch aromatic ester; 729 cm⁻¹,
08 benzene derivative (79)). (C) EDX spectrum of nylon, confirming the presence of carbon
09 (C), nitrogen (N) and oxygen (O). (D) μFTIR spectrum of nylon with characteristic nylon
10 absorbance peaks (3302 cm⁻¹, N-H stretch; 2934 cm⁻¹, C-H stretch; 1632 cm⁻¹, C=O
11 stretch sec. amide; 1202 cm⁻¹, C-N bend (79)).

12

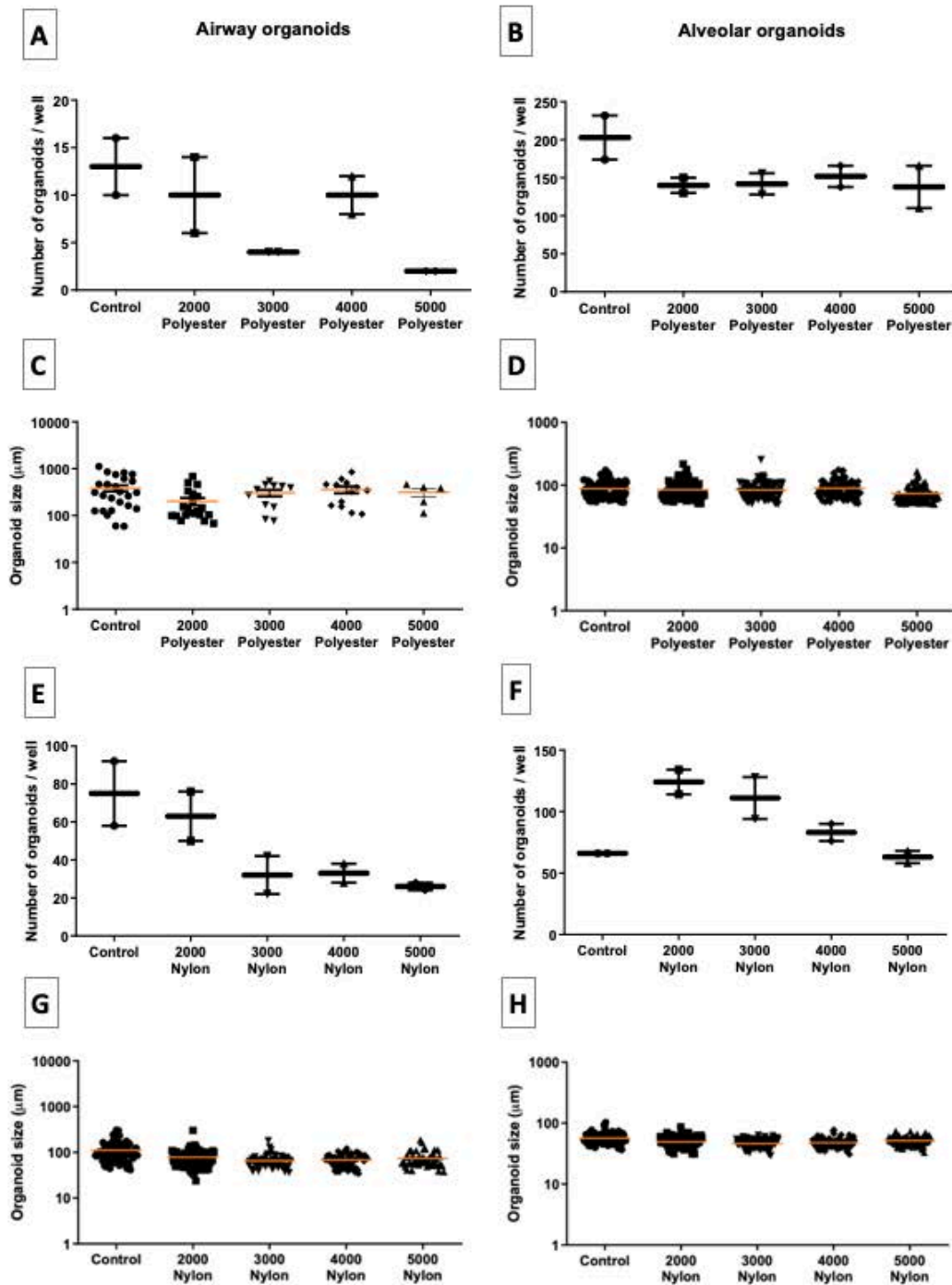


Figure S2: Determination of the optimal microfiber dose for subsequent in vitro testing of polyester and nylon reference microfibers, using 2000, 3000, 4000 and 5000 microfibers per condition. (A, E) Quantification of airway and (B, F) alveolar organoid numbers for organoids exposed to polyester or nylon, respectively ($n=2$ independent isolations). (C, G) Quantification of the airway and (D, H) alveolar organoid size following exposure to polyester or nylon. 2000, 3000, 4000 or 5000 fibers per well corresponded to approximately 49, 73, 98 and 122 $\mu\text{g}/\text{ml}$ of polyester fibers or 16, 23, 31, and 39 $\mu\text{g}/\text{ml}$ of nylon fibers.

22

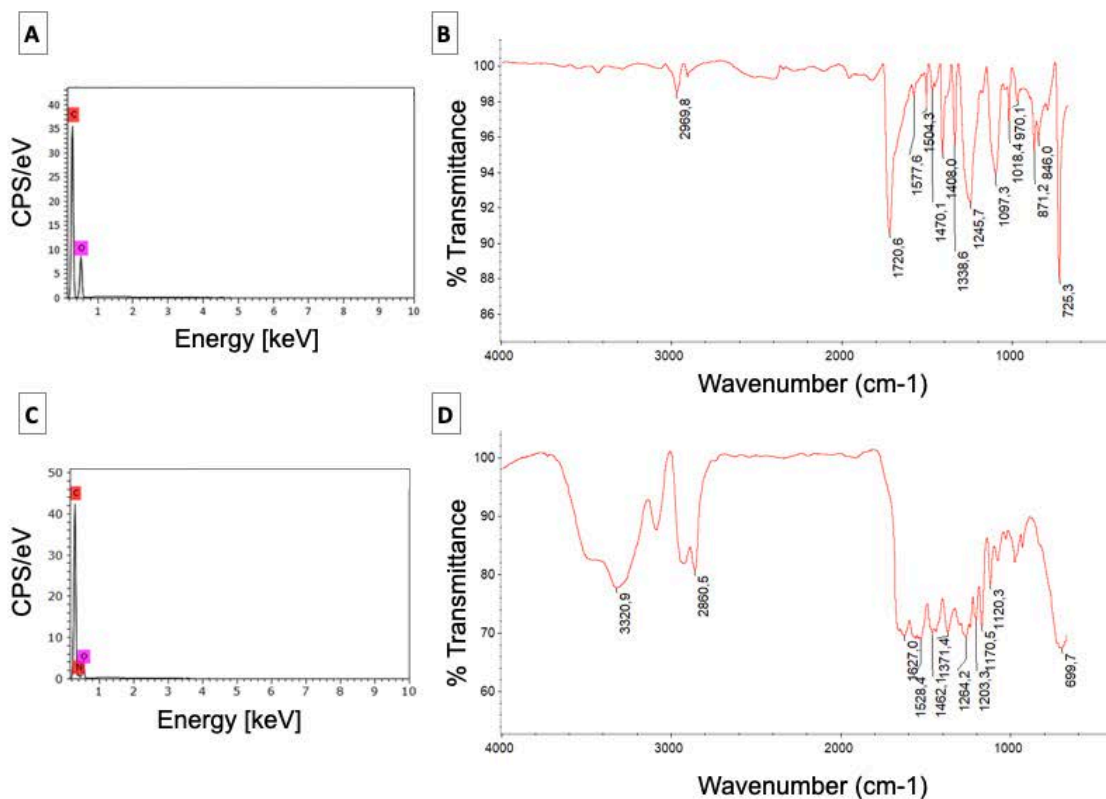
Table S2. Size characteristics of polyester and nylon environmental microfibers.

	Microfiber size Diameter x length (µm)	
	Environmental polyester	Environmental nylon
25% percentile	15x54	46x15
Median	17x63	57x20
75% percentile	18x85	73x27
Minimum	8x30	17x8
Maximum	24x269	296x66

23

24

25



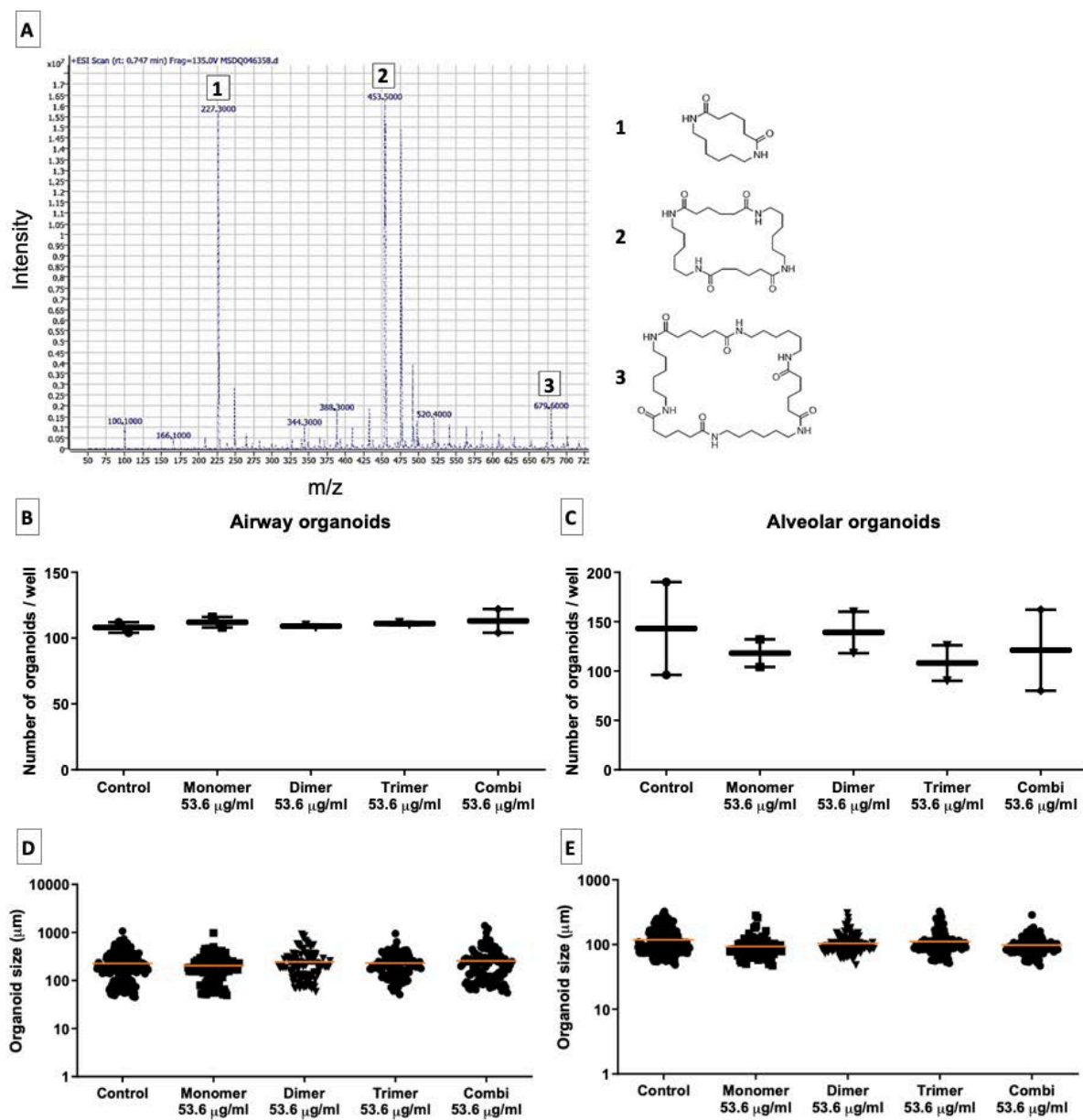
26

27

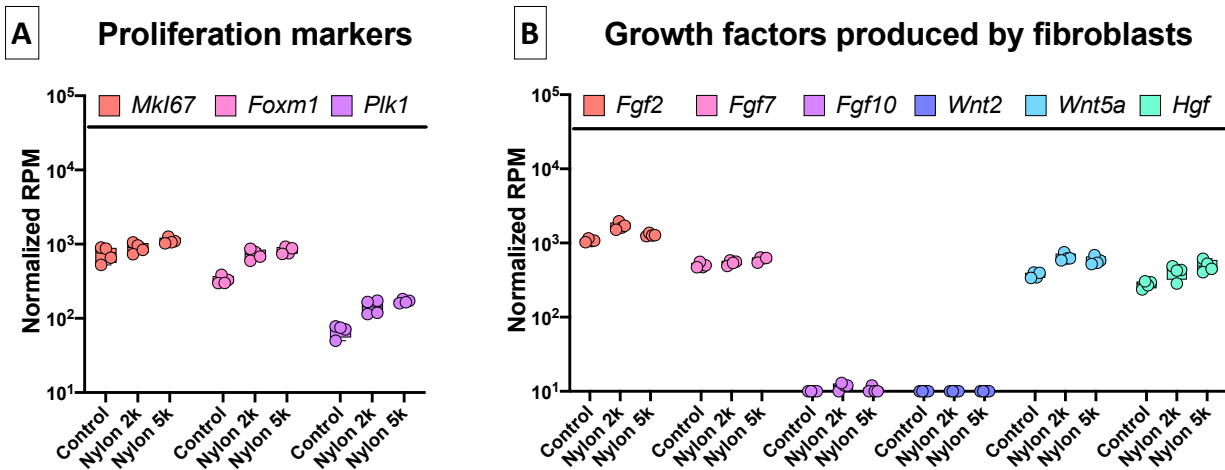
28

29

Figure S3: Characterization of the environmental microfibers using energy dispersive X-ray - and infrared spectroscopy. EDX - and μ -FTIR spectra of (A and B) polyester and (C and D) nylon microfibers.



30
31 **Figure S4: Characterization of the components leaching from nylon reference**
32 **microfibers and their effect on organoid growth.** (A) Mass spectrometry spectrum of the
33 nylon leachate, revealing high amounts of cyclic nylon mono-, di- and trimers, as well as
34 other smaller peaks. (B and C) Assessment of the numbers of airway and alveolar
35 organoids and (D and E) their sizes ($n=2$ independent isolations).



39

40

41

42

43

44

45

Figure S5: Expression of individual genes in fibroblasts isolated from organoid cultures exposed to nylon microfibers. (A) Genes associated with proliferation of fibroblasts. (B) Genes encoding factors produced by fibroblasts important for epithelial development (n=4 independent isolations). 2k= 2000 fibers, 5k=5000 fibers